Time-Dependent Density-Functional Theory (TD-DFT) with deMon2k: ASESMA Exercises

deMon stands for *densité* **de Mon***tréal*. For obvious reasons, the unofficial deMon logo is a demon or devil, mostly just for fun. This is a picture of Jun Maekawa's devil which is one of the most famous origami devils.

Mark Earl CASIDA
Laboratoire de Spectrométrie, Interactions et Chimie théorique (SITh), Département de Chimie Moléculaire (DCM, UMR CNRS/UGA 5250), Institut de Chimie Moléculaire de Grenoble (ICMG, FR2607), Université Grenoble Alpes (UGA) 301 rue de la Chimie, BP 53, F-38041 Grenoble Cedex 9, FRANCE
e-mail: mark.casida@univ-grenoble-alpes.fr

Date of Publication: May 30, 2025 (MS 0.12)

Contents

Chapter 1

Introduction

1.1 Acknowledgement

> "It takes a village to raise a child." — an African proverb originating in the Nigerian Igbo and Yaruba communities

These hands-on lessons are the product of a long-time participation in the deMon community. deMon stands for the French *densité de Montréal* (density of Montreal) because it originated in the PhD work of Alain ST-AMANT when he was a student of Dennis R. SALAHUB. The deMon program was one of the first gaussian-type orbitals (GTOs) density-functional theory (DFT) programs that could borrow sophisticated algorithms from *ab initio* (meaning Hartree-Fock and post-Hartree-Fock) methods to be able to perform geometry optimizations and, ultimately, *ab initio* dynamics calculations. I arrived in Montreal (Quebec, Canada) at this time as a senior scientist and computer support personnel. My job was, among other things, to help the students, postdocs, and many visiting scientists who came to use the deMon code. Since then, the deMon code developers community has dispersed around the world but still gets together annually to share, to take-stock-of, and to coordinate program development. More recently, the deMon developer meetings have become associated with deMon tutorials where we reach out to teach the program to a larger community. I am deeply indebted to this community for the program that we are using today and especially to Dennis R. SALAHUB, to Andreas KÖSTER, and to Gerald GEUDTNER.

deMon

GTO, DFT

I have also had the immense priviledge to teach and lead projects in many (but not all) of the African School on Electronic Structure Methods and Applications (ASESMA) over the years. It is my sincere opinion that these are the best summer schools for advanced learning that I have ever experienced and I use ASESMA as a model whenever called upon to help in the organization of other summer schools. The present notes are, in part, based upon a workbook (referred to here as just Workbook 1[1, 2]) that I prepared for various reasons, but not the least of which was to use in ASESMA and in collaborations that originated in ASESMA. In this sense, I would also like to acknowledge my deep debt to both ASESMA and to the African community of theoretical physicists and chemists for motivating me to prepare the present notes.

ASESMA

1.2 Preface

These hands-on lessons have been prepared for the ASESMA that took place in Accra, Ghana, in June 2025.

The *nominal* objective is

> "to learn a bit about how time-dependent (TD) DFT works" TD, deMon2k

in a program such as deMon2k designed for molecules. But the *real* objective is

> "to learn about static and nondynamical correlation as well as how chemical physicists think about molecules."

Traditionally ASESMA has focused on solid-state physics using periodic quantum physics codes. Quantum chemistry codes for molecules share many of the same principles that underlie periodic codes but with some differences which are partly historical and partly due to an emphasis on solving different types of problems. Let us develop this a little more.

A distinction is sometimes made between chemical physics and physical chemistry. Both are at the interface between chemistry and physics and so it can be hard (and not necessarily even desirable) to distinguish one from the other. Traditionally chemical physics was done in physics departments and physical chemistry was done in chemistry departments. However a perusal of the table of contents of the American Institute of Physics (AIP) *Journal of Chemical Physics* shows that many chemical physicists are chemistry department faculty. What is going on? I think that the AIP best explanation was given by the Rowlinson [3] who simply pointed out that the mathematics of traditional physical chemistry was adequate for thermodynamics, kinetics, and ion transport, but was relatively elementary compared to the mathematics routinely used in quantum mechanics. Hence, although, quantum mechanics is clearly the best way to model molecules, such work was traditionally relegated to physics departments until sometime in the 1970s. At that time, in the USA, quantum mechanics became well-established in physical chemistry courses and theoretical chemical physicists where hired in chemistry departments to do quantum mechanics. We had, in fact, reached the state where there is very little difference between chemical physics and physical chemistry and the identity of these two terms is even recognized in the name of the journal *Physical Chemistry Chemical Physics* PCCP (PCCP) published by the Royal Society of Chemistry.

What distinction remains between chemical physics and physical chemistry might best be answered by the somewhat flippant answer of a graduate student to whom I had posed the question of the difference when I was looking for an apopropriate school for graduate studies:

> "The difference between the two is whether you do the fun part first or save it for last."

Of course, he did not specify which part is the fun part (and I am sure that varies from person to person!) On a more serious note, chemistry is traditionally centered on chemical reactions. As such it is primiarly concerned about how atoms move, with the behavior of electrons in molecules as a secondary concern which can help understand chemical reactivity. In contrast, physicists seem less concerned with chemical reactions and more interested in the properties of molecules which are often determined by what the electrons do when perturbed by (possibly time-dependent) electronic or magnetic fields. (To be fair, it should be pointed out that chemists make heavy use of the physical properties of molecules in order to confirm that they have indeed synthesized their target product!)

Our purpose in these exercises is to explore strong correlation problems where a single determinantal (SDET) wave function is not enough. Such problems are omnipresent in describing excited states in molecules but are also important for describing ground state potential energy surfaces (PESs) or, as we will often focus on diatomics, potential energy curves (PECs). As a rule, our focus will be on multideterminantal (MDET) wave functions. We will also focus on simple systems—notably H_2—and use the freely downloadable executable of deMon2k which can easily be run on any personal computer running Linux. In this way, we hope that the student will continue to experiment and to learn from deMon2k, even after this ASESMA meeting.

SDET

PES, PEC

MDET

1.3 Molecular Orbital and Valence-Bond Theory

Let us explore some of the more delicate differences between (solid-state) physics and (quantum) chemistry. These differences are important because they reflect different thought processes motivated both by historical differences and by differences in how mental models are used in these two closely-related fields.

It has frequently been remarked that physics uses plane-wave basis sets while chemistry uses atom centered basis sets. This corresponds to the difference between three types of ideal bonding recognized by chemists. The first type is metallic bonding where the conduction electrons are free to move in the field of ions in a metal. This may be approximated by the homogeneous electron gas (HEG, also known as "jellium"), which is the old particle-in-a-box model with a uniform positive background to keep the system neutral and including electron correlation. Minimizing the jellium energy leads to a conduction electron density remarkably close to that of sodium metal, making sodium the closest real metal to the HEG.

HEG, jellium

Long ago, chemists developed an empirical model of two-electron bonding. This was further codified by the use of Lewis dot structures (LDSs) [4]. Note that we will use this term, even when not using dots to represent electrons. Hence [:N:::N:], [:N≡N:], and [N≡N] will all be called LDSs. (We will often put square brackets around our LDSs, though this is not a usual practice in chemistry.) As Lewis noted, this works equally well for describing covalent bonding and ionic bonding because ionic bonds are just extremely polar covalent bonds. LDSs are so deeply ingrained into chemical thinking that it is virtually impossible to work on, say, problems in organic electronics without knowing how to draw the LDSs of the molecules in the study.

LDS

Of course, metallic, covalent, and ionic bonding are just ideal cases. As emphasized, for example, by van Arkel's triangle [5, 6], all real bonds have mixed character. This is further emphasized by applications of the electron localization function (ELF) to lithium clusters [7]. The ELF uses concepts from DFT to reveal electron pairs in molecules. The ELF is localized between atoms for covalent bonds. It also reveals nonbonding lone pair electrons. However lithium clusters, Li_n, are expected to form a covalent bond for the dimer and to gradually show metallic bonding as n increases. In fact, the ELF shows that for many lithium clusters, the electron pairs are actually located in the

ELF

intersticies between groups of atoms, rather than as bonds and lone pairs. This, apparently is what metallic bonding looks like according to ELF.

The advent of quantum mechanics made it urgent to be able to describe bonding in molecules. Just one year after the publication of Schrödinger's famous paper [8, 9], Heitler and London published a paper which contained the valence-bond (VB) definition of the chemical in H_2 [10]. *This theory is all about spin coupling!* But let us proceed without equations for now. Heitler and London proposed that the wave function for H_2 could be written in two possible ways with one electron of each spin in an s atomic orbital (AO) on each atom, corresponding to the resonance structure [H$\uparrow$ $\downarrow$H $\leftrightarrow$ H$\downarrow$ $\uparrow$H]. This provided a qualitatively correct description of bonding and greatly pleased chemists who could see the electron pair bond of [H-H]. In fact, the resonance structures are identified with [H-H] in VB theory but dissociate into the proper atomic states at long bond distance. AO

Linus Pauling [11] began his career at the California Institute of Technology with the intention of using quantum mechanics to describe all of chemistry. As he was using VB theory, the wave function of H_2 was

$$\Psi = C_{\uparrow\downarrow}\Psi[\mathrm{H}\uparrow\ \downarrow\mathrm{H}] + C_{\downarrow\uparrow}\Psi[\mathrm{H}\downarrow\ \uparrow\mathrm{H}]\,, \tag{1.1}$$

so that the energy was (assuming real-valued wave functions),

$$\begin{aligned} E &= \langle\Psi|\hat{H}|\Psi\rangle \\ &= |C_{\uparrow\downarrow}|^2\langle\Psi[\mathrm{H}\uparrow\ \downarrow\mathrm{H}]|\hat{H}|\Psi[\mathrm{H}\uparrow\ \downarrow\mathrm{H}]\rangle + 2C_{\uparrow\downarrow}C_{\downarrow\uparrow}\langle\Psi[\mathrm{H}\uparrow\ \downarrow\mathrm{H}]|\hat{H}|\Psi[\mathrm{H}\downarrow\ \uparrow\mathrm{H}]\rangle \\ &+ |C_{\downarrow\uparrow}|^2\langle\Psi[\mathrm{H}\downarrow\ \uparrow\mathrm{H}]|\hat{H}|\Psi[\mathrm{H}\downarrow\ \uparrow\mathrm{H}]\rangle\,. \end{aligned} \tag{1.2}$$

However Pauling and his student George W. Wheland [12, 13, 14] were not only interested in quantitative calculations but also in communicating useful concepts that chemists could use to understand chemical structure and reactivity. In so doing, they took the VB model and described it diagrammatically by using resonance structures. Regrettably, they did a slight disservice by simplifying the energy expression to,

$$E = \langle\Psi|\hat{H}|\Psi\rangle \approx |C_{\uparrow\downarrow}|^2\langle\Psi[\mathrm{H}\uparrow\ \downarrow\mathrm{H}]|\hat{H}|\Psi[\mathrm{H}\uparrow\ \downarrow\mathrm{H}]\rangle + |C_{\downarrow\uparrow}|^2\langle\Psi[\mathrm{H}\downarrow\ \uparrow\mathrm{H}]|\hat{H}|\Psi[\mathrm{H}\downarrow\ \uparrow\mathrm{H}]\rangle\,, \tag{1.3}$$

in their verbal descriptions. Wheland struggled to make the resonance concept crystal clear:

> "the newer concepts can be made clearer with the aid of an analogy. A mule is a hybrid between a horse and a donkey. This does not mean that some mules are horses and the rest are donkeys, nor does it mean that a given mule is a horse part of the time and a donkey the rest of the time. Instead, it means that a mule is a new kind of animal, neither horse nor donkey, but intermediate between the two and partaking to some extent of the character of each. Similarly, the theories of intermediate stages and of mesomerism picture the benzene molecule as having a *hybrid* structure, not identical with either of the Kekulé structures, but intermediate between them." — p. 3 of Ref. [12].

Judging from his use of different analogies at different times [14], Wheland was probably not completely happy with any of these explanations. Certainly the "mule = donkey + horse" explanation of resonance in chemistry is wrong because expectation values necessarily contain cross terms.

Molecular orbital (MO) theory was a competing theory for describing the electronic structure of molecules. MOs were typically constructed as linear combinations of atomic orbitals, thereby defining the LCAO approximation. Because MO theory used a SDET of orthonormal MOs, it was much easier for doing calculations than was VB theory which required the use of linear combinations of several SDETs of nonorthonormal AOs. Furthermore, the number of possible resonance structures MO, LCAO that needed to be taken into account in VB theory seemed to explode in going to large molecules (i.e., the $N!$ problem of VB theory). For example, VB theory must also include the ionic structures [$\text{H:}^-\ \text{H}^+ \leftrightarrow \text{H}^+\ \text{:H}^-$] in the case of H_2. This is why almost all calculations (including DFT calculations!) are done these days using MO theory.

However VB theory is still very much alive as anyone who has a General Chemistry textbook can attest. While it is true that MO theory is invariably used to describe the electronic structure of diatomics (and the paramagnetism of O_2 is heralded as a victory of MO over VB theory even though Wheland showed how VB theory also predicts paramagnetism [15]), VB hybrid orbitals and bonding concepts are also introduced and resonance structures abound! Moreover, unbeknownst to most chemists, the highly mathematical subject of spin-coupling underlies their VB theory (e.g., [16]), and the only way to explain why benzene resonance structures whose π bonds cross are forbidden is because these structures are actually based upon the Rumer method of spin coupling [17].

World War II is often used as an arbitrary division between classical VB and modern VB theory. With this division the Coulson-Fischer proof of the equivalence of VB and MO configuration interaction (CI) theory falls just barely into the catagory of modern VB theory [18]. Modern VB theory has overcome many of the old problems of classical VB theory and is now roughly competitive with MO theory [19, 20, 21]. This is not the place to go into modern VB theory. *However VB ideas are extremely useful for the analysis of the dissociation of the ground and excited states of H_2.* And we shall not hesitate to use it for this purpose. CI

1.4 Molecular Hydrogen, H_2

The simplest molecule is H_2^+ but the simplest neutral molecule is H_2 for which the potential energy curves are well-known. For example, the following figure is from Ref. [22, 23]:

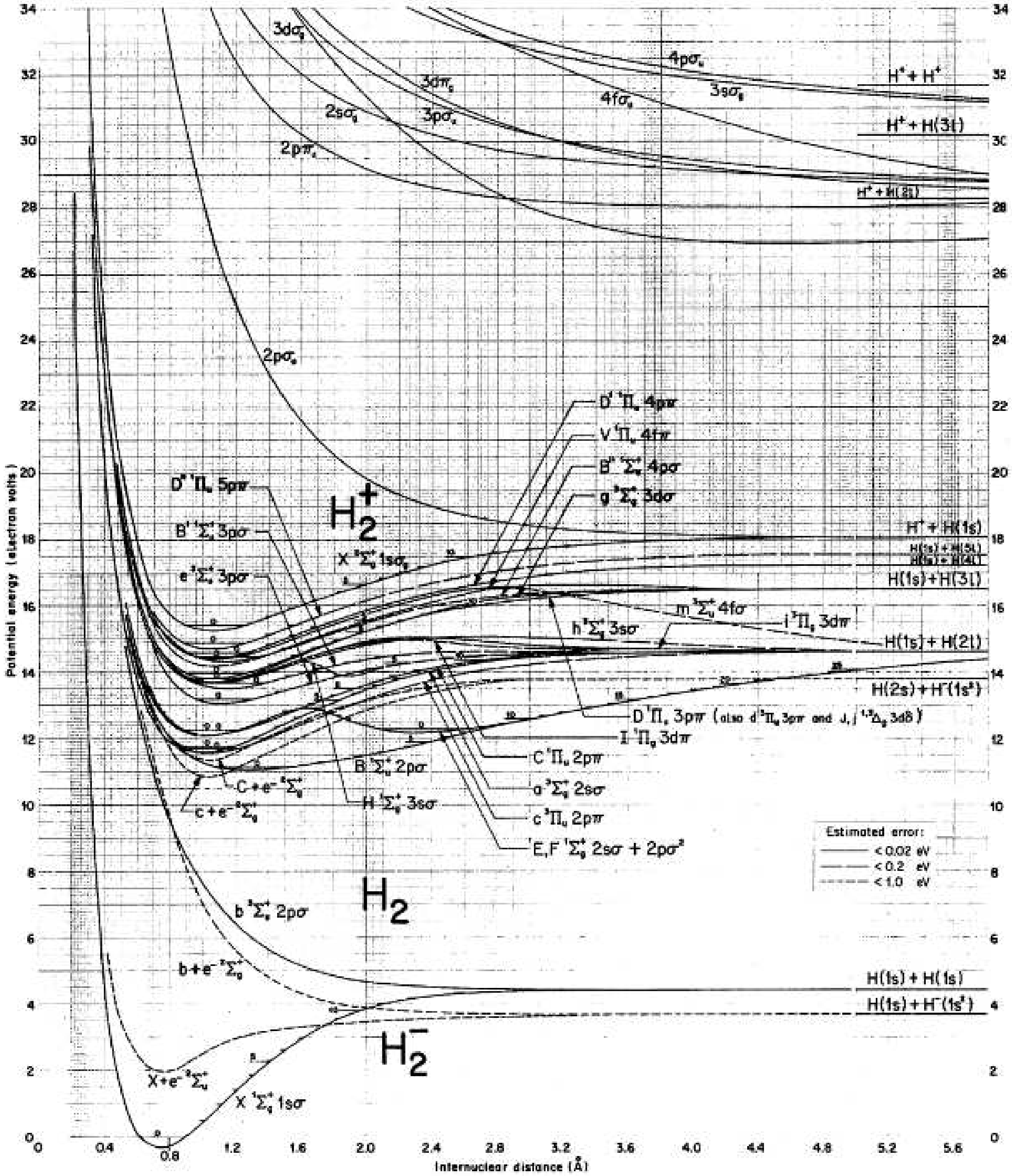

FIG. 2. Potential-Energy Curves for H_2^-, H_2, and H_2^+
A large-scale pullout of this drawing appears at the front of this issue
In general $1s\sigma$ has been omitted from state designations in order to save space

Note that this graph contains curves not only for H_2 but also curves for H_2^- and for H_2^+. In general, the more electrons, the lower the energy.

Because of time limitations, we will not try to calculate all of the PECs but will instead focus on the ground state $X\,^1\Sigma_g$, the first triplet state $a\,^3\Sigma_u$, and two excited states $B\,^1\Sigma_u$ and $E,F\,^1\Sigma_g$. We will be especially interested in the shapes of the PECs and in how H_2 dissociates for the different states. From the graph, the dissociation of the $X\,^1\Sigma_g$ and $a\,^3\Sigma_u$ states is to form [H↑ ↓H ↔ H↓ ↑H], while the dissociation of the $B\,^1\Sigma_u$ and $E,F\,^1\Sigma_g$ states is to form [H:$^-$ H$^+$ ↔ H$^+$:H$^-$]. We will just use the local density approximation (LDA) in its Vosko-Wilk-Nusair (VWN) parameterization [24] and only moderately-sized basis sets. LDA, VWN

Accurate PECs from the work of Kołos and Wolniewicz [25, 26, 27, 28, 29, 30, 31, 32, 33, 34] are given in the following table (obtained by digitizing Fig. 1 of Ref. [35]):

	Potential Energy Curves/Ha			
R/bohr	$X\,^1\Sigma$	$b\,^3\Sigma_u$	$B\,^1\Sigma_u$	$E,F\,^1\Sigma_g$
0.0				
0.1				
0.2				
0.3				
0.4				
0.5	0.45307			
0.6	0.22525			
0.7	0.07491			
0.8	-0.02493			
0.9	-0.08672	0.44505		
1.0	-0.12603	0.38554	0.41482	
1.1	-0.14969	0.32183	0.37067	0.38259
1.2	-0.16419	0.28854	0.33657	0.34815
1.3	-0.17129	0.24684	0.31334	0.32451
1.4	**-0.17404**	**0.22004**	**0.29425**	**0.30936**
1.5	-0.17254	0.19490	0.28030	0.29829
1.6	-0.16849	0.17150	0.26977	0.29100
1.7	-0.16240	0.15029	0.26169	0.28650
1.8	-0.15503	0.13191	0.25565	0.28408
1.9	-0.14695	0.11617	0.25131	0.28335
2.0	-0.13836	0.10254	0.24815	0.28378
2.1	-0.12928	0.09088	0.24637	0.28518
2.2	-0.12027	0.08002	0.24467	0.28737
2.3	-0.11155	0.07028	0.24382	0.29000
2.4	-0.10266	0.06237	0.24356	0.29297
2.5	-0.09417	0.05439	0.24364	0.29626
2.6	-0.08610	0.04761	0.24383	0.29956
2.7	-0.07840	0.04179	0.24457	0.30285
2.8	-0.07113	0.03654	0.24547	0.30582
2.9	-0.06423	0.03181	0.24648	0.30835
3.0	-0.05778	0.02769	0.24769	0.31025

$R_e = 1.4$ bohr
$D_e = 0.17404$ Ha
triplet excitation energy $E(b\,^2\Sigma_u) - E(X\,^1\Sigma) = 0.39408$ Ha
singlet excitation energy $E(B\,^1\Sigma_u) - E(X\,^1\Sigma) = 0.46829$ Ha
spin multiplet splitting $E(B\,^1\Sigma_u) - E(b\,^3\Sigma_u) = 0.07421$ Ha
$E(E,F\,^1\Sigma_g) - E(X\,^1\Sigma) = 0.48340$ Ha

	Potential Energy Curves/Ha			
R/bohr	$X\,^1\Sigma$	$b\,^3\Sigma_u$	$B\,^1\Sigma_u$	$E,F\,^1\Sigma_g$
3.1	-0.05177	0.02409	0.24900	0.31094
3.2	-0.04621	0.02093	0.25041	0.31021
3.3	-0.04114	0.01818	0.25197	0.30777
3.4	-0.03646	0.01573	0.25361	0.30480
3.5	-0.03225	0.01349	0.25532	0.30152
3.6	-0.02844	0.01157	0.25715	0.29820
3.7	-0.02517	0.01000	0.25905	0.29522
3.8	-0.02209	0.00862	0.26093	0.29264
3.9	-0.01940	0.00735	0.26276	0.29054
4.0	-0.01698	0.00629	0.26464	0.28888
4.1	-0.01484	0.00528	0.26675	0.28761
4.2	-0.01294	0.00435	0.26878	0.28675
4.3	-0.01125	0.00371	0.27094	0.28625
4.4	-0.00977	0.00317	0.27296	0.28616
4.5	-0.00857	0.00257	0.27508	0.28631
4.6	-0.00753	0.00216	0.27701	0.28682
4.7	-0.00650	0.00166	0.27923	0.28740
4.8	-0.00564	0.00136	0.28139	0.28824
4.9	-0.00499	0.00116	0.28349	0.28935
5.0	-0.00434	0.00090	0.28561	0.29056
5.1	-0.00384	0.00055	0.28769	0.29181
5.2	-0.00333	0.00039	0.28974	0.29328
5.3	-0.00322	0.00034	0.29180	0.29503
5.4	-0.00287	0.00014	0.29385	0.29689
5.5	-0.00282	-0.00006	0.29586	0.29868
5.6	-0.00281	-0.00011	0.29784	0.30049
5.7	-0.00269	-0.00019	0.29993	0.30343
5.8	-0.00245	-0.00037	0.30196	0.30430
5.9	-0.00237	-0.00039	0.30556	0.30611
6.0	-0.00237	-0.00017	0.30567	0.30793

Potential Energy Curves/Ha				
R/bohr	$X\,^1\Sigma$	$b\,^3\Sigma_u$	$B\,^1\Sigma_u$	$E,F\,^1\Sigma_g$
6.1	-0.00237	0.00018	0.30944	0.30982
6.2	-0.00237	-0.00042	0.30955	0.31126
6.3	-0.00237	-0.00020	0.31137	0.31207
6.4	-0.00237	-0.00020	0.31321	0.31287
6.5	-0.00237	-0.00020	0.31510	0.31368
6.6	-0.00237	-0.00020	0.31685	0.31489
6.7	-0.00237	-0.00020	0.31870	0.31653
6.8	-0.00237	-0.00019	0.32043	0.31813
6.9	-0.00237	-0.00017	0.32211	0.31975
7.0	-0.00237	-0.00031	0.32382	0.32142
7.1	-0.00237	-0.00052	0.32546	0.32308
7.2	-0.00237	-0.00052	0.32702	0.32461
7.3	-0.00237	-0.00048	0.32861	0.32628
7.4	-0.00237	-0.00052	0.33024	0.32795
7.5	-0.00237	-0.00048	0.33177	0.32951
7.6	-0.00237	-0.00048	0.33331	0.33086
7.7	-0.00237	-0.00048	0.33477	0.33212
7.8	-0.00237	-0.00048	0.33632	0.33352
7.9	-0.00237	-0.00048	0.33773	0.33510
8.0	-0.00237	-0.00060	0.33913	0.33678

We will refer to these values as EXACT. EXACT

Chapter 2

Exercises

2.1 Installation

This section is taken essentially verbatim from Workbook 1 [1, 2]. Note that we will *not* be downloading the free executable of deMon2k from the website as we want to use a more up-to-date version.

deMon2k should run under most Unix operating systems. If you do not have a computer running Unix, it is possible to run Unix on top of Windows on a personal computer (PC) or on top of the Apple operating system. An appendix in Workbook 1 explains how Nabila Oozeer installed Unix on her Mac notebook without removing the Apple operating system.

Unix, Windows, Apple, PC

Let us assume that you have succeeded in finding or creating a Unix environment. Let us see how you can install deMon2k on your machine by looking at how I installed it on my machine. Specifically I installed a binary version on my portable computer which runs CentOS Linux. Installation involved several steps:

CentOS, Linux

1. Going to `http://www.demon-software.com/public_html/download/binary/download.html?`

2. Filling in the form:

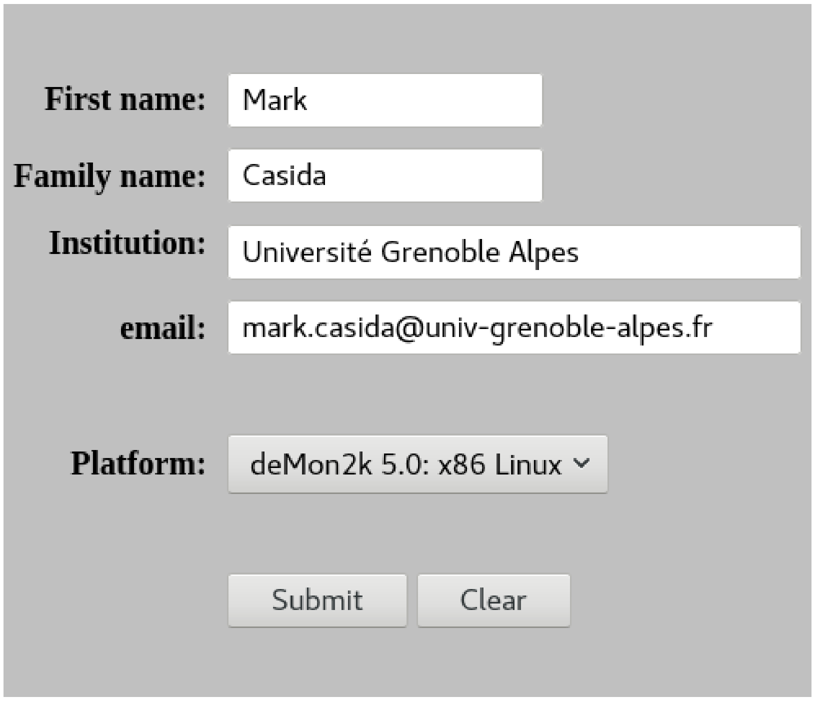

3. Creating a suitable directory for unpacking:

```
/home/mcasida/ENGINEERING/workbook/deMon->ls
deMon2k.5.0.x86_linux.tgz
```

4. Changing to that directory and unpacking it:

```
> cd /home/mcasida/ENGINEERING/workbook/deMon
> gunzip deMon2k.5.0.x86_linux.tgz
> ls
deMon2k.5.0.x86_linux.tar
>tar xvf deMon2k.5.0.x86_linux.tar
AUXIS
BASIS
binary
ECPS
FFDS
MCPS
> ls
AUXIS  BASIS  binary  deMon2k.5.0.x86_linux.tar  ECPS  FFDS  MCPS
```

   The executable is the file called `binary`. There are also several other files: `BASIS` contains a library of orbital basis sets, `AUXIS` contains a library of auxiliary basis sets for fitting the charge density and exchange correlation (xc) terms, `ECPS` and `MCPS` contain effective core potentials and model core potentials (two very similar concepts) respectively, and `FFDS` contains force field parameters for molecular modeling.

   BASIS, AUXIS, xc, ECPS, MCPS, FFDS

5. Creating a simple input file `deMon.inp` containing:

```
TITLE O2 (Basis: GEN-A3*/6-311++G**)
MULTI 3
#
VXCTYPE VWN
#
PRINT MOS
VISUALIZATION MOLDEN FULL
#
# --- GEOMETRY ---
#
#
GEOMETRY CARTESIAN ANGSTROM
O     0.000000    0.000000    0.603500
O     0.000000    0.000000   -0.603500
```

This is a single point calculation for the O_2 molecule in its triplet ground state using the LDA.

6. Run the program directly in the directory with the binary:

```
> ./binary < deMon.inp >& deMon.out
> ls
AUXIS  binary                     deMon.inp  deMon.mol  deMon.out  ECPS  MCPS
BASIS  deMon2k.5.0.x86_linux.tar  deMon.mem  deMon.new  deMon.rst  FFDS
> vi deMon.out
```

The program ran correctly, creating several additional files, including the main output in `deMon.out`, a restart file `deMon.rst`, one used for molecular visualization `deMon.mol`, and the files `deMon.meme` and `deMon.new`. The program seems to be working just fine.

2.2 Running the Program

This section is taken verbatim from Workbook 1 [1, 2].

Right now you have a directory (which I will call the `deMon_root` directory) which contains your executable, `BASIS` directory, `AUXIS` directory, etc. For various reasons, you do not want to run in the `deMon_root` directory. Instead, it is convenient to create a SHELL program (which I call `run.csh`) to run DEMON2K for you and do any clean up you might want to do afterwards. This section provides a simple example of how this is done.

`deMon_root`, SHELL, `run.csh`

Note that the ending `run.csh` indicates that this program is written in C SHELL (`csh`). Other options are possible, but I like C SHELL. My program is intended to be small and easily modifiable so that, once you understand it, you can adjust it to your own purposes and start to build your own SHELL programs.

`csh`

My program may be run in any directory of your account. It will look for a DEMON2K input file named `xxx.inp` in the same directory where "xxx" can be pretty much anything. Since DEMON2K always reads input from a file called `deMon.inp`, the file `xxx.inp` will have to be copied to `deMon.inp`. Also `run.csh` will have to copy the DEMON2K executable and any essential directories to the present directory. The job is then run. Once the job has finished, the output file `deMon.out` is renamed

`deMon.inp`, `deMon.out`

xxx.out (same "xxx" as for xxx.inp) and all the unimportant files are removed. In order to keep things simple, run.csh runs DEMON2K in foreground.

Here is the contents of run.csh which I have placed in the directory /home/mcasida/ENGINEERING/TDDFT/examples.

```
#!/bin/csh
# The previous line indicates that this is a C-shell file
# --------------------------------------------------------
# Program to run deMon in the present working directory.
# To use: Create an input file with the name xxx.inp where
# xxx can be anything.  Execute with
# /home/mcasida/ENGINEERING/TDDFT/examples/run.csh xxx
# The job runs interactively in foreground.
# --------------------------------------------------------
set xxx = $1
echo "Input file "$xxx.inp
set PWD = `pwd`
echo "The present working directory is "$PWD
set deMon_root = /home/mcasida/ENGINEERING/workbook/deMon2kv6p3 # location of deMon files
echo "Using directories and excecutables from "$deMon_root
#
# copy essential files to the present working directory
#
cp $deMon_root/BASIS $PWD # copy the BASIS file to the run directory
cp $deMon_root/AUXIS $PWD # copy the AUXIS file to the run directory
cp $deMon_root/binary $PWD/deMon.x # copy the executable to the run directory
cp $xxx.inp deMon.inp
#
# run deMon
#
./deMon.x
#
# clean up
\rm  BASIS
\rm  AUXIS
mv deMon.out $xxx.out
\rm deMon.*
# -------------
# End of file
# -------------
```

Note that comments begin with the "number sign" (#) except for the first line in run.csh which tells my computer that this is a csh program. The program needs to be made executable:

```
> chmod ugo+x run.csh
```

Let us see how the program works. I have copied the input file from Sec. 2.1 to the directory /home/mcasida/ENGINEERING/TDDFT/examples/Lesson0 as the file O2.inp. Here is a transcript of my session:

```
> ls
O2.inp
> cat O2.inp
TITLE O2 (Basis: GEN-A3*/6-311++G**)
MULTI 3
#
VXCTYPE VWN
#
PRINT MOS
VISUALIZATION MOLDEN FULL
#
# --- GEOMETRY ---
#
#
GEOMETRY CARTESIAN ANGSTROM
O     0.000000    0.000000    0.603500
O     0.000000    0.000000   -0.603500
> /home/mcasida/ENGINEERING/workbook/examples/run.csh O2
Input file O2.inp
The present working directory is /home/mcasida/ENGINEERING/workbook/examples/Lesson0
Using directories and excecutables from /home/mcasida/ENGINEERING/workbook/deMon
> ls
O2.inp  O2.out
```

In addition to the input file `O2.inp`, I now have my output file `O2.out` but nothing else. This is enough to get us started.

2.3 Getting the Code

Should you want to have a copy of the deMon2k FORTRAN code and you are an academic user (as opposed to someone in a company), then it suffices to go to FORTRAN

`http://www.demon-software.com/public_html/download.html`

and to follow the instructions. In particular, the *academic license* is simply a non-dissemination agreement saying that you agree not to share the code with anyone else. There is no charge but signing and returning the agreement helps the deMon developers to keep track of who is using the code, why, and where, which can be very useful information when seeking grant funding. As the web page says,

> "To obtain the source code of the deMon2k program, it is necessary to sign a license agreement. License agreements must be signed by people responsible for their own research groups. For further information please contact Dr. Patrizia Calaminici (e-mails: pcalamin@cinvestav.mx and calaminicipatrizia@gmail.com). The academic license is free of charge."

On the other hand, if you are part of a company who wants to use this program, there is a nominal charge for access to the code (please see the web page). In the past, money gained through non-academic licenses has been used to help finance a post-doc or to defray some of the costs of deMon developers meetings.

2.4 Vertical Excitations

Let us start by examining the minimum energy geometry of H_2 and what the excited states look like at this geometry. This will allow us to discuss several aspects of MDET calculations.

2.4.1 Atomic Units

Before going any further, it is important to discuss units. We will be using Hartree atomic units for convenience. Hartree atomic units are based upon the Gaussian system of electromagnetic units where Maxwell's equations have the form,

$$\begin{aligned} \vec{\nabla} \cdot \vec{E} &= 4\pi\rho(\vec{r}) \\ \vec{\nabla} \times \vec{E} &= -\frac{1}{c}\frac{\partial \vec{B}}{\partial t} \\ \vec{\nabla} \cdot \vec{B} &= 0 \\ \vec{\nabla} \times \vec{B} &= \frac{4\pi}{c}\vec{\jmath}(\vec{r}) + \frac{1}{c}\frac{\partial \vec{E}}{\partial t} \,. \end{aligned} \tag{2.1}$$

This may be compared with Maxwell's equations in *Système internationale* (SI) units, SI

$$\begin{aligned} \vec{\nabla} \cdot \vec{E} &= \frac{\rho(\vec{r})}{\epsilon_0} \\ \vec{\nabla} \times \vec{E} &= -\frac{1}{c}\frac{\partial \vec{B}}{\partial t} \\ \vec{\nabla} \cdot \vec{B} &= 0 \\ \vec{\nabla} \times \vec{B} &= \mu_0\vec{\jmath}(\vec{r}) + \mu_0\epsilon_0\frac{\partial \vec{E}}{\partial t} \\ \mu_0\epsilon_0 &= \frac{1}{c^2} \,. \end{aligned} \tag{2.2}$$

The presence of μ_0 and ϵ_0 in SI units means that SI units actually have one more fundamental dimension than is the case in Gaussian units—hence the historical preference for Gaussian units in theoretical work. Furthermore charges and magnetic fields have different dimensionality in the two systems of units. These is easiest to see if we neglect the magnetic field ($\vec{B} = \vec{0}$). Then Coulomb's law in Gaussian units is,

$$F = \frac{q_1 q_2}{r_{1,2}} \,, \tag{2.3}$$

and in SI units is,

$$F = \frac{Q_1 Q_2}{(4\pi\epsilon_0) r_{1,2}} \,. \tag{2.4}$$

Evidently,

$$Q = \sqrt{4\pi\epsilon_0} q \,, \tag{2.5}$$

for most of the applications that we are likely to encounter.

Hartree atomic units begin with the Gaussian system of electromagnetic units and set $\hbar = m_e = e = 1$ atomic unit. In this system, the units of distance and energy are,

$$\begin{aligned} 1 \text{ bohr} &= a_0 = \frac{\hbar^2}{m_e e^2} = 0.529 \text{ Å} \\ 1 \text{ hartree} &= 1 \text{ Ha} = E_h = \frac{\hbar^2}{m_e a_0^2} = 27.2 \text{ eV} = 219{,}000 \text{ cm}^{-1} = 628 \text{ kcal/mol} \,. \end{aligned} \tag{2.6}$$

(As a side note, $c = 137.03599$ atomic units is curiously close to exactly 137.) *It is very important to realize that some programs use Rydberg atomic units.* These are the same as Hartree atomic units, except that the energy unit is the rydberg (Ry): 1 Ha = 2 Ry; 1 Ry = 0.5 Ha. Ha, Ry

2.4.2 Basis Sets

This section is taken essentially verbatim from Workbook 1 [1, 2].

LCAO approximation It is well-known that the many-body problem cannot be solved exactly and so approximations are needed. However physicists (by which I generally mean solid-state physicists who are used to doing periodic calculations on metals and semiconductors) and chemists (by which I generally mean physical chemists/chemical physicists who are used to doing calculations on molecules) typically build their approximations based upon different physical pictures. For a physicist, the first approximation is that of an idealized metal where the wave functions of the conduction electrons are plane waves. These plane waves are delocalized over physical (x, y, z) space but localized in momentum space and lend themselves to Fourier transform methods. For a chemist, on the other hand, molecules are thought of as made up of atoms which interact to make bonding MOs, nonbonding MOs, and antibonding MOs. The simplest approximation is that each MO is the LCAO approximation. Although this is only a first approximation to more accurate descriptions of the electronic structure of molecules, it is still at the heart of much of chemical thinking. Each MO ψ_i is expanded in terms of AOs χ_μ as,

$$\begin{aligned} \psi_i(\vec{r}) &= \sum_\mu \chi_\mu(\vec{r}) C_{\mu,i} \\ \left(\begin{array}{ccc} \psi_1(\vec{r}) & \psi_2(\vec{r}) & \cdots \psi_n(\vec{r}) \end{array} \right) &= \left(\begin{array}{ccc} \chi_1(\vec{r}) & \chi_2(\vec{r}) & \cdots \chi_m(\vec{r}) \end{array} \right) \left[\begin{array}{cccc} C_{1,1} & C_{1,2} & \cdots & C_{1,n} \\ C_{2,1} & C_{2,2} & \cdots & C_{2,n} \\ \vdots & \vdots & \ddots & \vdots \\ C_{m,1} & C_{m,2} & \cdots & C_{m,n} \end{array} \right], \end{aligned} \tag{2.7}$$

where the $C_{\mu,i}$ are referred to as MO coefficients. Notice how Latin indices are used for MOs and Greek indices are used for AOs. This is a very consistent practice throughout the Quantum Chemistry literature. Also capital Latin and Greek letters (such as Ψ) are reserved for many-electron quantities while small Latin and Greek letters (such as ψ) are reserved for 1-electron (e.g., MO) quantities, but there are some exceptions as capital letters are frequently used for matrices for historical reasons.

Each AO is naturally enough centered on an atom (often referred to as a "center"). True AOs on any given center are orthonormal (or, more exactly, may be chosen to be orthonormal),

$$S_{\mu,\nu} = \langle \chi_\mu | \chi_\nu \rangle = \int \chi_\mu^*(\vec{r}) \chi_\nu(\vec{r})\, d\vec{r} = \delta_{\mu,\nu} = \left\{ \begin{array}{lll} 1 & \text{if} & \mu = \nu \\ 0 & \text{if} & \mu \neq \nu \end{array} \right. . \tag{2.8}$$

However AOs from different atoms are *not* orthonormal and chemists are used to visualizing how the AOs interact:

$$S_{\mu,\nu} \left\{ \begin{array}{lll} > 0 & \Rightarrow & \text{bonding} \\ = 0 & \Rightarrow & \text{nonbonding} \\ < 0 & \Rightarrow & \text{antibonding} \end{array} \right. \tag{2.9}$$

This is adequate to describe the simple AO/MO correlation diagrams found in first-year University chemistry courses (e.g., Fig. 2.1.)

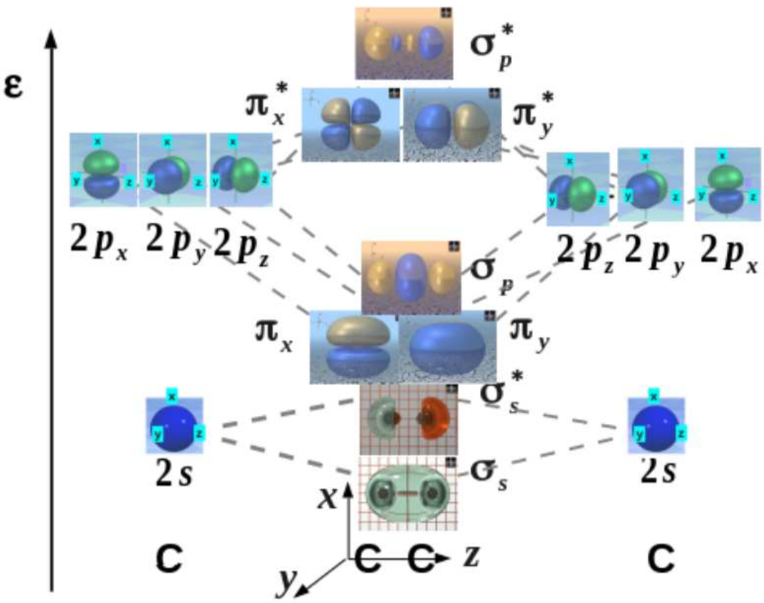

Figure 2.1: Part of the solution to last year's final exam in the first-year course (CHI 131) that I teach. Notice how AOs with $S > 0$ come together to create MOs with lower energy than the corresponding AOs (i.e., are bonding) while AOs with $S < 0$ come together to create MOs with higher energy than the corresponding AOs (i.e., are antibonding).

Dirac-Roothaan Representation Sometimes it is useful to use a more compact representation. This is made possible using Dirac's bras and kets. The bras and kets are related to the wavefunctions by,

$$
\begin{aligned}
\psi(\vec{r}) &= \langle \vec{r} | \psi \rangle \\
\phi^*(\vec{r}) &= \langle \phi | \vec{r} \rangle .
\end{aligned}
\tag{2.10}
$$

Then,

$$
\begin{aligned}
\langle \phi | \psi \rangle &= \int \phi^*(\vec{r}) \psi(\vec{r}) \, d\vec{r} \\
&= \int \langle \phi | \vec{r} \rangle \langle \vec{r} | \psi \rangle \, d\vec{r} \\
&= \langle \phi | \left(\int | \vec{r} \rangle \langle \vec{r} | \, d\vec{r} \right) | \psi \rangle .
\end{aligned}
\tag{2.11}
$$

Note how this implies the completeness relation,

$$\hat{1} = \int |\vec{r}\rangle\langle\vec{r}| \, d\vec{r} . \tag{2.12}$$

In bra-ket notation, Eq. (2.7) is written as,

$$|\psi_i\rangle = \sum_\mu |\chi_\mu\rangle C_{\mu,i} , \tag{2.13}$$

or,

$$\vec{\psi}^\dagger = \vec{\chi}^\dagger \mathbf{C}\,, \tag{2.14}$$

where,

$$\begin{aligned}
\vec{\psi}^\dagger &= \begin{pmatrix} |\psi_1\rangle & |\psi_2\rangle & \cdots |\psi_n\rangle \end{pmatrix} \\
\vec{\chi}^\dagger &= \begin{pmatrix} |\chi_1\rangle & |\chi_2\rangle & \cdots |\chi_m\rangle \end{pmatrix} \\
\mathbf{C} &= \begin{bmatrix} C_{1,1} & C_{1,2} & \cdots & C_{1,n} \\ C_{2,1} & C_{2,2} & \cdots & C_{2,n} \\ \vdots & \vdots & \ddots & \vdots \\ C_{m,1} & C_{m,2} & \cdots & C_{m,n} \end{bmatrix} .
\end{aligned} \tag{2.15}$$

Similarly,

$$\begin{aligned}
\vec{\phi} &= \begin{pmatrix} \langle\psi_1| \\ \langle\psi_2| \\ \ddots \\ \langle\psi_n| \end{pmatrix} \\
\vec{\chi} &= \begin{pmatrix} \langle\chi_1| \\ \langle\chi_2| \\ \ddots \\ \langle\chi_m| \end{pmatrix} .
\end{aligned} \tag{2.16}$$

I call this combination of Dirac notation and matrix notation "Dirac-Roothaan notation" because the first time I saw it was in an article by Roothaan. This allows us to write some things very compactly:

$$\begin{aligned}
\mathbf{S} = \vec{\chi}\vec{\chi}^\dagger &\Rightarrow \text{Overlap matrix} \\
\mathbf{H} = \vec{\chi}\hat{h}\vec{\chi}^\dagger &\Rightarrow \text{Orbital Hamiltonian matrix} \\
\hat{P} = \vec{\chi}^\dagger \mathbf{S}^{-1}\vec{\chi} &\Rightarrow \text{Resolution-of-the-identity}\,.
\end{aligned} \tag{2.17}$$

Note that the resolution-of-the-indentity (RI) only gives the identity operator, $\hat{1}$, in the limit of a complete basis set. Nevertheless, *assuming* that the RI projector is the identity operator provides a quick way to find the matrix form of the orbital equation that can be found more rigorously from the variational principle. This equation is solved in deMon2k and other quantum chemistry programs:

$$\begin{aligned}
\hat{h}|\psi_i\rangle &= \epsilon_i|\psi_i\rangle \\
\vec{\chi}\hat{h}\hat{P}|\psi_i\rangle &= \epsilon_i\vec{\chi}|\psi_i\rangle \\
\vec{\chi}\hat{h}\vec{\chi}^\dagger\mathbf{S}^{-1}\vec{\chi}|\psi_i\rangle &= \epsilon_i\vec{\chi}|\psi_i\rangle \\
\mathbf{H}\vec{C}_i &= \epsilon_i\mathbf{S}\vec{C}_i\,,
\end{aligned} \tag{2.18}$$

where,

$$\vec{C}_i = \mathbf{S}^{-1}\vec{\chi}|\psi_i\rangle\,, \tag{2.19}$$

is the ith column of the matrix $\mathbf{C}$ of MO coefficients because,

$$\begin{aligned}
|\psi_i\rangle &= \vec{\chi}^\dagger\vec{C}_i \\
\vec{\chi}|\psi_i\rangle &= \vec{\chi}\vec{\chi}^\dagger\vec{C}_i \\
\vec{\chi}|\psi_i\rangle &= \mathbf{S}\vec{C}_i \\
\vec{C}_i &= \mathbf{S}^{-1}\vec{\chi}|\psi_i\rangle\,.
\end{aligned} \tag{2.20}$$

One nice thing about the Dirac-Roothaan representation is that it provides useful tools for dealing with basis sets which are *not* orthonormal, which is almost always the case in quantum chemistry.

It is worth repeating that the matrix form of the orbital equation solved in most quantum chemistry program is,

$$\mathbf{H}\vec{C}_i = \epsilon_i \mathbf{S}\vec{C}_i \,, \tag{2.21}$$

which is a sort of generalized eigenvalue problem. It is often solved using Lödwin's method which involves taking the square root of the overlap matrix:

$$\begin{aligned} \mathbf{H}\mathbf{S}^{-1/2}\mathbf{S}^{+1/2}\vec{C}_i &= \epsilon_i \mathbf{S}^{+1/2}\mathbf{S}^{+1/2}\vec{C}_i \\ \left(\mathbf{S}^{-1/2}\mathbf{H}\mathbf{S}^{-1/2}\right)\left(\mathbf{S}^{+1/2}\vec{C}_i\right) &= \epsilon_i \left(\mathbf{S}^{+1/2}\vec{C}_i\right) \\ \tilde{\mathbf{H}}\tilde{C}_i &= \epsilon_i \tilde{C}_i \,, \end{aligned} \tag{2.22}$$

where objects indicated with a tilde are sometimes called the symmetrized quantities,

$$\begin{aligned} \tilde{\mathbf{H}} &= \mathbf{S}^{-1/2}\mathbf{H}\mathbf{S}^{-1/2} \\ \tilde{C}_i &= \mathbf{S}^{+1/2}\vec{C}_i \,. \end{aligned} \tag{2.23}$$

A final calculation is then needed to retrieve the true MO coefficients,

$$\vec{C}_i = \mathbf{S}^{-1/2}\tilde{C}_i \,. \tag{2.24}$$

Gaussian-type Orbitals The LCAO approximation is only a starting point for accurate approximations which use more elaborate basis sets. There are many excellent reviews of the basis sets used in quantum chemistry (e.g., Ref. [36, 37]). These should be studied. My goal here is only to give a minimal overview.

Although some programs (e.g., DMol [38]) actually start with real atomic orbitals obtained from atomic calculations on many-electron atoms, most programs take a different approach. DMol

True AOs look roughly like hydrogen atom orbitals which take the familiar form,

$$\chi_{n,l,m}(\vec{r}) = Y_{l,m}(\theta,\phi) R_{n,l}(r) \,, \tag{2.25}$$

where the radial function is a polynomial times an exponential. For example,

$$\begin{aligned} R_{1s}(r) &= 2\left(\frac{Z}{a_0}\right)^{3/2} e^{-Zr/a_0} \\ R_{2s}(r) &= \frac{1}{\sqrt{2}}\left(\frac{Z}{a_0}\right)^{3/2}\left(1-\frac{Zr}{2a_0}\right) e^{-Zr/a_0} \\ R_{2p}(r) &= \frac{1}{2\sqrt{6}}\left(\frac{Z}{a_0}\right)^{5/2} r e^{-Zr/a_0} \,, \end{aligned} \tag{2.26}$$

where a_0 is the Bohr radius and Z is the atomic number of the 1-electron atom. As the nodes in the radial wave function are due to the requirement that the higher energy orbitals be orthogonal to the lower energy orbitals and as this orthogonalization emerges naturally in variational calculations, it is enough to use Slater-type orbitals (STOs) of the form, STO

$$\chi_{n,l,m}(\vec{r}) \propto Y_{l,m}(\theta,\phi) r^{n-1} e^{-\zeta r/a_0} \,. \tag{2.27}$$

In many-electron atoms, the real atomic number Z is replaced by an effective atomic number ζ (Greek letter *zeta*) which may, for example, be determined by Slater's rules [39]. The problem with spherical-harmonic STOs in the form of Eq. (2.27) is that these STOs are complex valued which is a problem both for visualization and because it increases computation times. However spherical-harmonic orbitals may be made the real and imaginary parts if necessary,

$$
\begin{aligned}
Y_{0,0} &= \frac{1}{2\sqrt{\pi}} \\
Y_{1,0} &= \frac{1}{2}\sqrt{\frac{3}{\pi}}\frac{z}{r} \\
\Re e Y_{1,1} &= \frac{1}{2}\sqrt{\frac{3}{2\pi}}\frac{x}{r} \\
\Im m Y_{1,1} &= \frac{1}{2}\sqrt{\frac{3}{2\pi}}\frac{y}{r} \, .
\end{aligned}
\tag{2.28}
$$

This allows the spherical STOs to be replaced by cartesian STOs of the form,

$$
\chi_{l_x,l_y,l_z}(\vec{r}) \propto x^{l_x} y^{l_y} z^{l_z} e^{-\zeta r/a_0} \, . \tag{2.29}
$$

Here $l = l_x + l_y + l_z$ is more or less the azimuthal quantum number except that certain combinations actually lead to functions of lower azimuthal quantum number. For example, there is no $d_{x^2+y^2+z^2}$ function because $x^2 + y^2 + z^2 = r^2$ is spherically symmetric, hence an s function. STOs are used in some programs, such as ADF [40], electron repulsion integrals involving more than two centers are difficult to evaluate using STOs. ADF

Instead it is better to use GTOs of either the spherical-harmonic or cartesian type. These differ from STOs by the replacement $\exp(-\zeta r/a_0)$ by $\exp(-\alpha r^2/a_0^2)$ to make primitive GTOs,

$$
\chi_{l_x,l_y,l_z}(\vec{r};\alpha) \propto x^{l_x} y^{l_y} z^{l_z} e^{-\alpha r^2/a_0^2} \, . \tag{2.30}
$$

Fixed linear combinations of primitive GTOs make contracted GTOs of the form,

$$
\chi_{\mu}(\vec{r}) \propto x^{l_x} y^{l_y} z^{l_z} \sum_i e^{-\alpha_i r^2/a_0^2} d_i \, . \tag{2.31}
$$

Here the d_i are the contraction coefficients and the α_i are the exponentials. deMon2k uses a GTO basis set.

Contracted GTOs may resemble STOs as in the case of the STO-3G basis minimal basis set where each STO is approximated by a linear combination of three primitive GTOs. Note that a *minimal basis set* corresponds to the case where there is one orbital for each core and for each valence orbital (whether the latter are occupied or not). This partly justifies the common practice of referring to GTOs as AOs.

One criticism which is sometimes made of GTOs by physicists who are used to planewave codes is that there is no single parameter (like the wave number cut-off) that can be used to control the convergence of the basis set. It is possible to control the convergence of a GTO basis set in a systematic way by using, for example, even-tempered Gaussians which are known to provide a uniform coverage of the function space and by systematically enlarging the angular degree of freedom by increasing the largest azimuthal quantum number l in the basis set. However this is rarely done because chemists usually want the *smallest* basis set which is adequate for studying the molecular

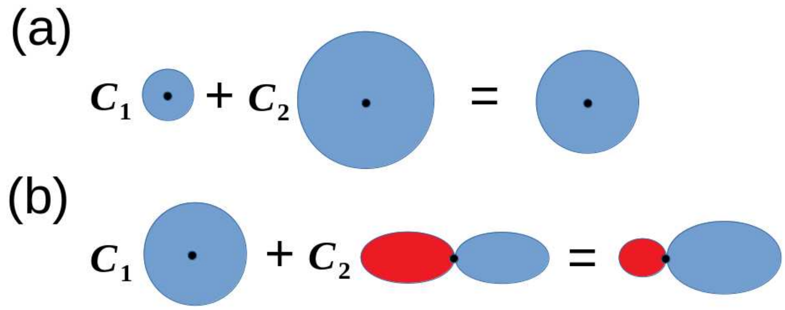

Figure 2.2: Illustration of the effects of using (a) a double ζ basis set and (b) a polarization function.

system (or systems) of interest to them. So the usual strategy is to expand the minimal basis set in two ways.

The first way is to double or triple (double ζ or triple ζ) the number of AOs (i.e., really GTOs) so as to allow expansion or contraction of the AO by variational optimization of, for example, a linear combination of a smaller and a larger GTO of the same type (Fig. 2.2a.) The second way is to include polarization functions of higher angular momentum than in the minimal basis which may be used to describe an angular deformation of an atom or polarization of a bond (Fig. 2.2b.) Clearly these tight or diffuse or polarization functions are no longer atomic orbitals, but it is still common practice to call them AOs.

A convenient place to find GTO basis sets is at the **Basis Set Exchange**: `https://www.basissetexchange.org/`. You can even download GTO basis sets specifically in deMon2k format!

BASIS file The deMon2k `BASIS` file is a library of orbital basis sets. For example, for the hydrogen atoms, the file includes the following orbital basis sets:

1. O-HYDROGEN HYDROGEN H (41) (DZV) (DZV-LDA)
2. O-HYDROGEN HYDROGEN H (41/1) (DZVP) (DZVP-LDA) [41]
3. O-HYDROGEN HYDROGEN H (DZV-GGA)
4. O-HYDROGEN HYDROGEN H (DZVP-GGA) [42]
5. O-HYDROGEN HYDROGEN H (41/11*) (TZVP)
6. O-HYDROGEN HYDROGEN H (3) (STO-3G) [43]
7. O-HYDROGEN HYDROGEN H (6-31G**) [44, 45]
8. O-HYDROGEN HYDROGEN H (6-311G**) [46]
9. O-HYDROGEN HYDROGEN H (DEF2-TZVPP) [47]
10. O-HYDROGEN HYDROGEN H (3111/11) (EPR) (EPR-III) [48]
11. O-HYDROGEN HYDROGEN H (311/1) (IGLO-II) [49]

12. O-HYDROGEN HYDROGEN H (3111/11) (IGLO-III) [49]
13. O-HYDROGEN HYDROGEN H (LIC) [50]
14. O-HYDROGEN HYDROGEN H (SAD) [51]
15. O-HYDROGEN HYDROGEN H (41/1*) (TZVP-FIP1) [52]
16. O-HYDROGEN HYDROGEN H (41/1*/1+) (TZVP-FIP2) [52]
17. O-HYDROGEN HYDROGEN H (DZ-ANO) [53]
18. O-HYDROGEN HYDROGEN H (cc-pVTZ) [54]
19. O-HYDROGEN HYDROGEN H (AUG-CC-PVDZ) [55]
20. O-HYDROGEN HYDROGEN H (AUG-CC-PVTZ) [55]
21. O-HYDROGEN HYDROGEN H (AUG-CC-PVQZ) [55]
22. O-HYDROGEN HYDROGEN H (AUG-CC-PV5Z) [55]
23. O-HYDROGEN H (AUG-PCJ-0) [56]
24. O-HYDROGEN H (AUG-PCJ-1) [56]
25. O-HYDROGEN H (AUG-PCJ-2) [56]
26. O-HYDROGEN H (AUG-PCJ-3) [56]
27. O-HYDROGEN H (AUG-PCJ-4) [56]
28. O-HYDROGEN HYDROGEN H (LANL2DZ) [57]

It is also possible to input your own basis set (possibly one downloaded from the **Basis Set Exchange**) via the standard deMon2k input file.

Let us take a look at the format of one of these basis sets to get an idea of what the numbers mean:

```
O-HYDROGEN HYDROGEN H (SAD)
  5
  1  0   4
       33.8650140000        0.0060680000
        5.0947880000        0.0453160000
        1.1587860000        0.2028460000
        0.3258400000        0.5037090000
  2  0   1
        0.1027410000        1.0000000000
  3  0   1
        0.0324000000        1.0000000000
  2  1   2
        1.1588000000        0.1884400000
        0.3258000000        0.8824200000
```

```
 3  1   2
         0.1027000000          0.1178000000
         0.0324000000          0.0042000000
```

This is an example of a Sadlej field-induced polarisation basis which is specifically designed for efficient calculation of molecular polarizabilities. The number “5” after the title tells us that this basis set consists of 5 contracted GTOs. The next line “1 0 4” tells us the following lines describe the first (“1”) s-type ($l = 0$) function which is a contraction of 4 primitive GTOs. The exponents and contraction coefficients are:
$1s$

1. $\alpha_1 = 33.8650140000$, $d_1 = 0.0060680000$
2. $\alpha_2 = 5.0947880000$, $d_2 = 0.0453160000$
3. $\alpha_3 = 1.1587860000$, $d_3 = 0.2028460000$
4. $\alpha_4 = 0.3258400000$, $d_4 = 0.5037090000$

The line “2 0 1” announces the next basis function which is the second s-type function consisting of a single primitive GTO:
$1s'$

1. $\alpha_1 = 0.1027410000$, $d_1 = 1.0000000000$

The line “3 0 1” announces the third basis function which is the third s-type function consisting of a single primitive GTO:
$1s''$

1. $\alpha_1 = 0.0324000000$, $d_1 = 1.0000000000$

Figure 2.3 shows how the exponents form a rough geometric series. This is not an accident but instead a property that has to be satisfied when GTOs provide a uniform coverage of function space [58]. Continuing on to the next lines: The line “2 1 2” announces the first set of p-type functions consisting of the contraction of two primitive GTOs:
$2p_x, 2p_y, 2p_z$

1. $\alpha_1 = 1.1588000000$, $d_1 = 0.1884400000$
2. $\alpha_2 = 0.3258000000$, $d_2 = 0.8824200000$

This is followed by the line “3 1 2” which announces the second set of p-type functions which also consists of the contraction of two primitive GTOs:
$2p'_x, 2p'_y, 2p'_z$

1. $\alpha_1 = 0.1027000000$, $d_1 = 0.1178000000$
2. $\alpha_2 = 0.0324000000$, $d_2 = 0.0042000000$

The total size of the basis set is $m = 3$ s-type functions + 2 sets of 3 p-type functions = 9 AOs.

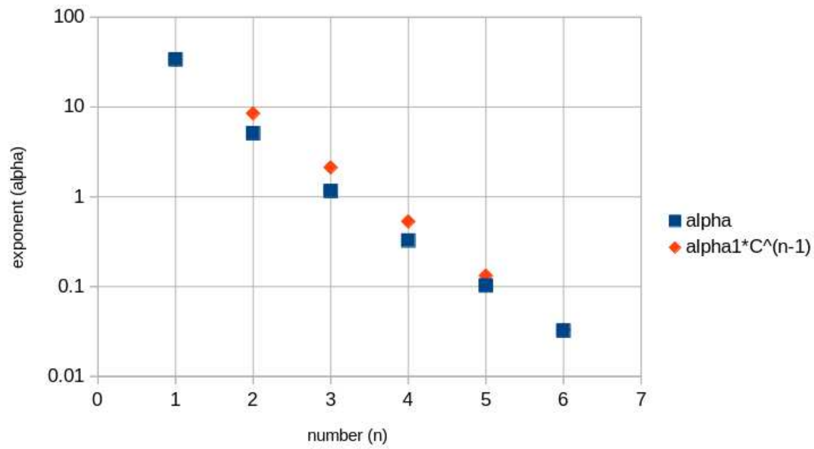

Figure 2.3: The exponents in the Sadlej basis set showing that they form a rough geometric series of the form $\alpha_n = \alpha_1 * (C^{n-1})$ where $C = 0.25$.

2.4.3 Dissociation Energy

The ground-state bond energy or dissociation energy D_e of H_2 is, D_e, D_0

$$D_e = 2E(\mathrm{H}) - E(\mathrm{H}_2)\,. \tag{2.32}$$

(When the zero-point vibrational energy is included, this quantity is known as D_0.) For some of the excited states, the dissociation energy is,

$$D_e = (E(\mathrm{H}^+ + E(\mathrm{H}^-)) - E(\mathrm{H}_2)\,. \tag{2.33}$$

It is clear that you must calculate the following energies: H^+, H, H^-, and H_2 at its equilibrium geometry. I recommend that you use a spread sheet (such as EXCEL or LIBREOFFICE CALC) to keep track of these energies. We will use the Sadlej basis set and many program defaults. *The first energies to calculate are the atomic energies.*

H^+ Copy the following input file and run deMon2k:

Contents of `Hplus.inp`

```
TITLE H+ (Basis: SAD/GEN-A3*)
CHARGE +1
MULTI 1
#
SCFTYPE UKS
VXCTYPE VWN
#
PRINT MOS
#
# --- GEOMETRY ---
#
#
```

```
GEOMETRY CARTESIAN BOHR
H     0.000000    0.000000    0.000000
#
AUXIS (GEN-A3*)
BASIS (SAD)
```

Note down:

1. The size of the basis set (number of AOs)
2. The total energy in Ha (hartrees)
3. The spin α and spin β orbital energies
4. Anything else you find interesting.

Discuss your results.

H Copy the following input file and run deMon2k:

Contents of `Hneut.inp`

```
TITLE H (Basis: SAD/GEN-A3*)
CHARGE 0
MULTI 2
#
SCFTYPE UKS
VXCTYPE VWN
#
PRINT MOS
#
# --- GEOMETRY ---
#
#
GEOMETRY CARTESIAN BOHR
H     0.000000    0.000000    0.000000
H     0.000000    0.000000    5.000000
#
AUXIS (GEN-A3*)
BASIS (SAD)
```

Note down:

1. The size of the basis set (number of AOs)
2. The total energy in Ha (hartrees)
3. The spin α and spin β orbital energies
4. Anything else you find interesting.

Discuss your results.

H^- Copy the following input file and run deMon2k:

Contents of `Hminus.inp`

```
TITLE H- (Basis: SAD/GEN-A3*)
CHARGE -1
MULTI 1
#
SCFTYPE UKS
VXCTYPE VWN
#
PRINT MOS
#
# --- GEOMETRY ---
#
#
GEOMETRY CARTESIAN BOHR
H     0.000000    0.000000    0.000000
#
AUXIS (GEN-A3*)
BASIS (SAD)
```

Note down:

1. The size of the basis set (number of AOs)
2. The total energy in Ha (hartrees)
3. The spin α and spin β orbital energies
4. Anything else you find interesting.

Discuss your results.

H_2 Obtaining the equilibrium energy of H_2 requires a geometry optimization. Copy the following input file and run deMon2k:

Contents of `H2opt.inp`

```
TITLE H2 (Basis: SAD/GEN-A3*)
CHARGE -1
MULTI 1
#
SCFTYPE UKS
OPTIMIZATION
VXCTYPE VWN
#
PRINT MOS
#
# --- GEOMETRY ---
```

```
#
#
GEOMETRY CARTESIAN BOHR
H     0.000000    0.000000    0.000000
#
AUXIS (GEN-A3*)
BASIS (SAD)
```

Note down:

1. Check that the calculations are correctly converged.
2. Determine the equilibrium bond length and total energy.
3. Determine the bond dissociation energy.
4. From an examination of the MO coefficients, sketch cartoons of the first 9 MOs at the equilibrium geometry.
5. Anything else you find interesting.

Discuss your results.

2.4.4 Excited States

There are various ways to treat excited states in DFT. We will examine a few of these here and then try to calculate the vertical excitation energies for a few states using a couple of different methods.

Textbook MO Model Every first-year University-level General Chemistry course discusses MO theory for at least a few homonuclear diatomic molecules, the first of which is typically H_2. Let us label the atoms: H_A-H_B. The atom is fixed in space and is traditionally oriented along the z-axis. Just as when studying crystals, symmetry is very important when studying small molecules in order to understand selection rules governing which orbitals are zero and which are nonzero. The H_2 molecule has axial symmetry (rotation around the z-axis leaves the molecule unchanged), has mirror symmetry [reflection around the (x, y) mirror plane (*plan mirroir* in French) bisecting the H-H axis leaves the molecule unchanged], and there is also a center of inversion symmetry in the middle of the bond. We will take the usual minimal basis of a single $1s$ orbital on each atom. The $1s$ AO on H_A will be referred to as s_A and the $1s$ AO on H_B will be referred to as s_B. According to group theory, the MOs must belong to irreducible representations (irreps) of the molecule. In the first instance, we will only be concerned with orbitals with cylindrical symmetry with respect to rotation around the bond axis (i.e., σ orbitals) and even or odd symmetry with respect to reflection through the center of inversion (same, in the present simple model, as refection through the mirror plane). We may make two MOs—namely, irrep

$$
\begin{aligned}
\sigma_g &= \frac{1}{\sqrt{2(1+S)}}(s_A + s_B) \\
\sigma_u &= \frac{1}{\sqrt{2(1-S)}}(s_A - s_B) \ ,
\end{aligned} \tag{2.34}
$$

where,

$$S = \langle s_A | s_B \rangle = \langle s_B | s_A \rangle \,, \tag{2.35}$$

is the overlap matrix. As written, the two MOs are orthonormal. They are used to construct the orbital correlation diagram (OCD): overlap matrix OCD

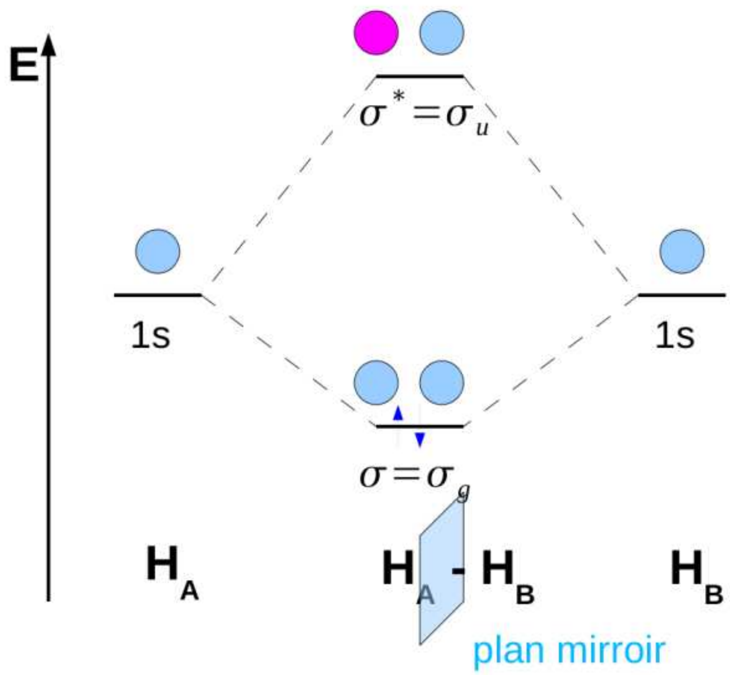

Notice that the MOs are always represented using lower case letters.

> *A long-standing tradition requires that, whenever possible, lower case Greek and Latin letters be used for orbital quantities, while upper case Greek and Latin letters are reserved for many-electron (state) quantities.*

The subscript g stands for *gerade* (even in German) while u states for *ungerade* (odd in German). The MO names σ_u and σ_g emphasize the symmetry. Most General Chemistry textbooks use σ for the bonding MO and σ^* for the antibonding MO. We prefer the symmetry notation.

We now have a two-orbital two-electron model (TOTEM) problem from which we wish to construct wave functions. The TOTEM is a (2/2) model where (n/m) refers to n electrons in m orbitals. There are several ways to occupy MOs in our TOTEM: TOTEM

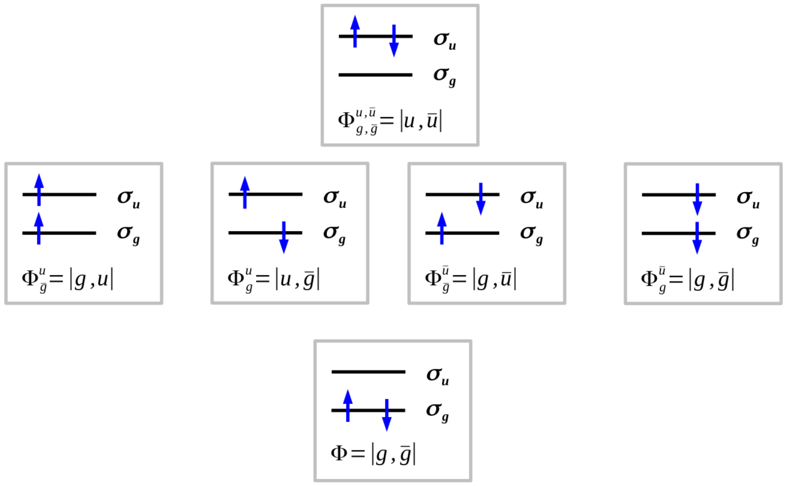

The state energies have been ordered using a zero-order estimate neglecting electron repulsions so that the energy is just given by the total of the orbital energies. Thus the lowest energy orbital is doubly occupied in the ground state and the highest energy orbital is doubly occupied in the highest energy excited state. In-between, we have four states which are energetically degenerate in the zero-order approximation. This is the famous *spin multiplet problem*. This is a common feature in molecular spectroscopy and photochemistry but is rarely studied in solid-state physics because of the complexity of spin-coupling Avogadro's number of electrons. Nevertheless it does come up in solid-state physics in the Kondo effect and in Josephson junctions. A full explanation of spin-coupling is quite complicated [17] and would take us too far away from our objectives. Fortunately, we will show that the situation is much easier when we only have two electrons because the 2-electron wave function factors into a space and a spin part. As the entire wave function must be antisymmetric, one but not both of the two factors into which the wave function separates must be antisymmetric while the other is symmetric. Let us see exactly how this happens. spin multiplet

Note that I use a short-hand notation for a Slater determinant, namely

$$\begin{aligned}|r,s| &= \frac{1}{\sqrt{2}}\begin{vmatrix}\phi_r(1) & \phi_s(1)\\ \phi_r(2) & \phi_s(2)\end{vmatrix}\\ &= \frac{1}{\sqrt{2}}\left(\phi_r(1)\phi_s(2)-\phi_s(1)\phi_r(2)\right)\,,\end{aligned}\tag{2.36}$$

where i stands for the coordinates of electron i. In addition $\bar{i}$ stands for the spatial orbital i times the β ($\downarrow$) spin function while i stands for the same thing except times the α ($\uparrow$) spin function. Therefore

$$\begin{aligned}|g,\bar{g}| &= \frac{1}{\sqrt{2}}\left(g(1)\alpha(1)g(2)\beta(2)-g(1)\beta(1)g(2)\alpha(2)\right)\\ &= \left(\sigma_g(1)\sigma_g(2)\right)\left[\frac{1}{\sqrt{2}}\left(\alpha(1)\beta(2)-\beta(1)\alpha(2)\right)\right]\,.\end{aligned}\tag{2.37}$$

(I am using g as synonymous with σ_g and similarly for u.) $|g,\bar{g}|$ is a Σ_g wave function because it is cylindrically symmetric around the bond axis and because it is even with respect to inversion symmetry. Similarly,

$$\begin{aligned}|u,\bar{u}| &= \frac{1}{\sqrt{2}}\left(u(1)\alpha(1)u(2)\beta(2)-u(1)\beta(1)g(2)\alpha(2)\right)\\ &= \left(\sigma_u(1)\sigma_u(2)\right)\left[\frac{1}{\sqrt{2}}\left(\alpha(1)\beta(2)-\beta(1)\alpha(2)\right)\right]\,,\end{aligned}\tag{2.38}$$

is also Σ_g (because odd $\times$ odd = even).

Now let us turn specifically to the spin multiplet states! Since,

$$
\begin{aligned}
|g,u| &= \frac{1}{\sqrt{2}}\left(g(1)\alpha(1)u(2)\alpha(2) - u(1)\alpha(1)g(2)\alpha(2)\right) \\
&= \left[\frac{1}{\sqrt{2}}\left(\sigma_g(1)\sigma_u(2) - \sigma_u(1)\sigma_g(2)\right)\right]\left(\alpha(1)\alpha(2)\right) \,, \qquad (2.39)
\end{aligned}
$$

then we have a Σ_u state. Also

$$
\begin{aligned}
|\bar{g},\bar{u}| &= \frac{1}{\sqrt{2}}\left(g(1)\beta(1)u(2)\beta(2) - u(1)\beta(1)g(2)\beta(2)\right) \\
&= \left[\frac{1}{\sqrt{2}}\left(\sigma_g(1)\sigma_u(2) - \sigma_u(1)\sigma_g(2)\right)\right]\left(\beta(1)\beta(2)\right) \,, \qquad (2.40)
\end{aligned}
$$

is a Σ_u state. However, neither $|u,\bar{g}|$ nor $|g,\bar{u}$ factor into the product of a spatial part and a spin part. Ultimately this is because they are not eigenstates of the $\hat{S}^2$ operator, though they are eigenstates of $\hat{S}_z$ with eigenvalue,

$$
M_S = \frac{n_\alpha - n_\beta}{2} \,, \qquad (2.41)
$$

which is zero for $\Phi_M = |u,\bar{g}|$ and for $\Phi_{\bar{M}} = |g,\bar{u}|$. Often we call them symmetry-mixed states or just mixed states. We can use them to create eigenstates of $\hat{S}^2$ by taking the normalized $\pm$ combinations: mixed states

$$
\begin{aligned}
\frac{1}{\sqrt{2}}\left(|u,\bar{g}| \pm |g,\bar{u}|\right) &= \frac{1}{2}\left(u(1)\alpha(1)g(2)\beta(2) - g(1)\beta(1)u(2)\alpha(2)\right) \pm \frac{1}{2}\left(g(1)\alpha(1)u(2)\beta(2) - u(1)\beta(1)g(2)\alpha(2)\right) \\
&= \left[\frac{1}{\sqrt{2}}\left(u(1)g(2) \pm g(1)u(2)\right)\right]\left[\frac{1}{\sqrt{2}}\left(\alpha(1)\beta(2) \mp \beta(1)\alpha(2)\right)\right] \,. \qquad (2.42)
\end{aligned}
$$

These are Σ_u states as well.

We now make use of the fact that we are neglecting all spin-orbit terms in our (electronic) hamiltonian,

$$
\begin{aligned}
\hat{H} &= \hat{h}(1) + \hat{h}(2) + \frac{1}{r_{1,2}} - \frac{1}{|\vec{r}_1 - \vec{R}_A|} \\
\hat{h} &= -\frac{1}{2}\nabla^2 - \frac{1}{|\vec{r} - \vec{R}_A|} - \frac{1}{|\vec{r} - \vec{R}_B|} \,. \qquad (2.43)
\end{aligned}
$$

Then a wave function $\Psi = \Psi_{\text{space}}\Psi_{\text{spin}}$ that factors into a space and a spin part has an energy which is independent of the spin part and so depends only on the space part,

$$
E = \langle\Psi|\hat{H}|\Psi\rangle = \langle\Psi_{\text{space}}|\hat{H}|\Psi_{\text{space}}\rangle \,. \qquad (2.44)
$$

Consequently, our multiplet spin problem resolves into a non-degenerate open-shell *singlet state*, singlet state

$$
\begin{aligned}
\Psi_{0,0} &= \frac{1}{\sqrt{2}}\left(|u,\bar{g}| + |g,\bar{u}|\right) \\
\Psi_{\text{space}}^{\text{singlet}} &= \frac{1}{\sqrt{2}}\left(\sigma_g(1)\sigma_u(2) + \sigma_u(1)\sigma_g(2)\right) \,, \qquad (2.45)
\end{aligned}
$$

and three energetically-degenerate triplet states,

vertical state

$$
\begin{aligned}
\Psi_{1,+1} &= |g,u| \\
\Psi_{1,0} &= \frac{1}{\sqrt{2}}\left(|g,\bar{u}| - |u,\bar{g}|\right) \\
\Psi_{1,-1} &= |\bar{g},\bar{u}| \\
\Psi_{\text{space}}^{\text{triplet}} &= \frac{1}{\sqrt{2}}\left(\sigma_g(1)\sigma_u(2) - \sigma_u(1)\sigma_g(2)\right) ,
\end{aligned} \tag{2.46}
$$

Here I have introduced the notation Ψ_{S,M_S} where S and M_S are spin quantum numbers,

$$
\begin{aligned}
\hat{S}^2\Psi_{S,M_S} &= S(S+1)\Psi_{S,M_S} \\
\hat{S}_z\Psi_{S,M_S} &= M_S\Psi_{S,M_S} .
\end{aligned} \tag{2.47}
$$

2.4.5 Spin-Coupling Theory

This section is taken essentially verbatim from Workbook 1 [1, 2]. There are no exercises, but simply has been added for the sake of completeness for those who might be curious.

So far the treatment of spin has been kept as elementary as possible, but this limits us to two-electron wave functions. Let us now try to give a more advanced treatment of spin. This treatment can be generalized to more than two spins where wave functions no longer factor into the product of a spatial and a spin part. Even in the two-electron case, it may help to make the structure of the spin problem more evident. We will skip many details which may be found in advanced textbooks, but there should be enough detail that the reader can follow and apply the basic ideas. We consider the case where we have N *unpaired* spins to place in N orbitals. In our two-electron problem, this corresponds to the case of placing one electron in each of the σ_g and σ_u orbitals.

The spin-coupling problem is of fundamental importance in the few-body problem and is closely linked to the Lie algebra treatment of continuous groups. Under these conditions, it is perhaps not surprising that many different ways have been invented to handle spin-coupling (e.g., Clebsch-Gordon coefficients, Young diagrams based upon the symmetric group, graphical unitary group treatment, etc.) The approach presented here is based upon ladder operators. The ladder operator treatment of angular momentum is treated in most graduate-level textbooks on quantum physics.

In the case of a single electron, we have the three basic spin operators $\hat{s}_x$, $\hat{s}_y$, and $\hat{s}_z$ which commute with our spin-less hamiltonian, but not with each other. Hence the three spin-components do *not* consititute a set of three simultaneous observables. They obey the cyclic commutation relations,

$$
\begin{aligned}
[\hat{s}_x, \hat{s}_y] &= i\hbar\hat{s}_z \\
[\hat{s}_z, \hat{s}_x] &= i\hbar\hat{s}_y \\
[\hat{s}_y, \hat{s}_z] &= i\hbar\hat{s}_x .
\end{aligned} \tag{2.48}
$$

In some sense, any set of three operators that obey these relations may be thought of as "angular momentum operators." All three of the basic spin operators commute with the total spin operator,

$$
\hat{s}^2 = \hat{s}_x^2 + \hat{s}_y^2 + \hat{s}_z^2 . \tag{2.49}
$$

As $\left[\hat{H}, \hat{s}_z\right] = \left[\hat{H}, \hat{s}^2\right] = [\hat{s}^2, \hat{s}_z] = 0$, quantum mechanics tells us that we may chose the simultaneious eigenvalues of $\hat{s}^2$ and of $\hat{s}_z$ as constants of motion,

$$
\begin{aligned}
\hat{s}^2\psi_{s,m_s} &= s(s+1)\hbar^2\psi_{s,m_s} \\
\hat{s}_z\psi_{s,m_s} &= m_s\hbar\psi_{s,m_s} .
\end{aligned} \tag{2.50}
$$

In particular, for a single electron, $s = 1/2$ and $m_s = \pm 1/2$, so we have

$$\begin{aligned}
\hat{s}^2\psi &= \frac{3}{4}\hbar^2\psi \\
\hat{s}_z\psi &= +\frac{1}{2}\hbar\psi \\
\hat{s}^2\bar{\psi} &= \frac{3}{4}\hbar^2\bar{\psi} \\
\hat{s}_z\bar{\psi} &= -\frac{1}{2}\hbar\psi \, .
\end{aligned} \tag{2.51}$$

It is also useful to define the raising operator,

$$\hat{s}_+ = s_x + is_y \, , \tag{2.52}$$

and the lowering operator,

$$\hat{s}_- = s_x - is_y \, . \tag{2.53}$$

It can be shown that

$$\begin{aligned}
\hat{s}_+\psi &= 0 \\
\hat{s}_+\bar{\psi} &= \hbar\psi \\
\hat{s}_-\psi &= \hbar\bar{\psi} \\
\hat{s}_-\bar{\psi} &= 0 \, .
\end{aligned} \tag{2.54}$$

We say that each pair $(\psi, \bar{\psi})$ forms a spin ladder which can be climbed with $\hat{s}_+$ and descended with $\hat{s}_-$.

In the case of N electrons, the spin operators generalize to,

$$\begin{aligned}
\hat{S}_x &= \sum_{i=1,N} \hat{s}_x(i) \\
\hat{S}_y &= \sum_{i=1,N} \hat{s}_y(i) \\
\hat{S}_z &= \sum_{i=1,N} \hat{s}_z(i) \, .
\end{aligned} \tag{2.55}$$

(Notice the use of capital letters since we are now dealing with many-electron quantities.) The definitions,

$$\begin{aligned}
\hat{S}^2 &= \hat{S}_x^2 + \hat{S}_y^2 + \hat{S}_z^2 \\
\hat{S}_+ &= \hat{S}_x + i\hat{S}_y \\
\hat{S}_- &= \hat{S}_x - i\hat{S}_z \, ,
\end{aligned} \tag{2.56}$$

still hold, but

$$\hat{S}^2 \neq \sum_{i=1,N} \hat{s}^2(i) \, . \tag{2.57}$$

This complicates the problem of constructing spin eigenfunctions. In general, for arbitary N, there will be several spin ladders. The precise number can be read of the spin-coupling diagram 2.4.

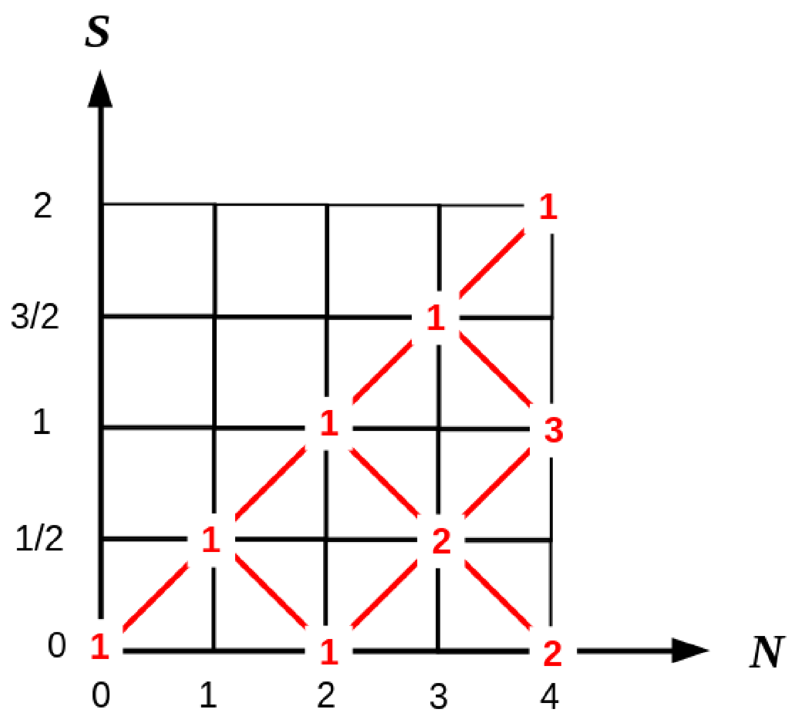

Figure 2.4: Spin-coupling diagram for counting the number of spin ladders as a function of the number of electrons. For example, for $N = 4$ electrons, there is one quintet ladder with $S = 2$, three triplet ladders with $S = 1$, and two singlet ladders with $S = 0$.

We will explain one method for constructing spin eigenfunctions and illustrate the method by applying it to the case of $N = 2$ electrons placed in the orbitals ψ and ϕ. This consists in beginning with the head of the spin ladder with the largest value of S which is always single determinantal and descending, knowing the general relations,

$$\begin{aligned} \hat{S}_+\Psi_{(S,M_S)} &= \hbar\sqrt{S(S+1)-M_S(M_S+1)}\Psi_{(S,M_S+1)} \\ \hat{S}_-\Psi_{(2S+1,M_S)} &= \hbar\sqrt{S(S+1)-M_S(M_S-1)}\Psi_{(S,M_S-1)} \,, \end{aligned} \tag{2.58}$$

where the complicated prefactor preserves normalization. Although not strictly necessary, I will rewrite key operators in second-quantized form.

In order to introduce second-quantized operators, let us abandon the overbar notation and work directly with spin-orbitals *for this paragraph only!* We will assume a spin-orbital basis of orthonormal orbitals. The effect of a creation operator $r^\dagger = \hat{a}_r^\dagger$ on a single determinant wave function $|s,t,u,v,\cdots|$ is to add another spin-orbital at the beginning of the determinant,

$$r^\dagger|s,t,u,v,\cdots| = |r,s,t,u,v,\cdots| \,. \tag{2.59}$$

The result is zero if r is already one of the spin-orbitals in the determinant. The adjoint of the creation operator is the corresponding annihilation operator $r = \hat{a}_r$ which undoes the operation of $r^\dagger$,

$$r|r,s,t,u,v,\cdots| = |s,t,u,v,\cdots| \,. \tag{2.60}$$

If the spin-orbital r is not in the beginning of the determinant list, then use antisymmetry to permute r to the beginning of the determinant list, keeping track of any sign changes. If the spin-orbital r is not in the list, then the action of r on the determinant is zero. It is then possible to deduce the following *anti*commutation rules:

$$\begin{aligned} [r,s]_+ &= \left[r^\dagger,s^\dagger\right]_+ = 0 \\ \left[r,s^\dagger\right]_+ &= \left[r^\dagger,s\right]_+ = \delta_{r,s} \,. \end{aligned} \tag{2.61}$$

Writing operators in second-quantized form provides an easy machinary for working with antisymmetric wave functions without having to think too much (which is why I like to use it.)

Let us return now to our usual notation and denote spin α ($\uparrow$) orbitals by r and spin β ($\downarrow$) orbitals by $\bar{r}$. It is now easy to write the operators,

$$\begin{aligned} \hat{n}_\uparrow &= \sum_r r^\dagger r \\ \hat{n}_\downarrow &= \sum_r \bar{r}^\dagger \bar{r} \,, \end{aligned} \tag{2.62}$$

that count the number of each type of spin in a determinant or a linear combination of determinants all with the same number of orbitals of each spin-type. Let us call this wave function, Ψ, then

$$\begin{aligned} \hat{n}_\uparrow\Psi &= n_\uparrow\Psi \\ \hat{n}_\downarrow\Psi &= n_\downarrow\Psi \,. \end{aligned} \tag{2.63}$$

From

$$M_S = \frac{n_\uparrow - n_\downarrow}{2} \,, \tag{2.64}$$

we have that

$$\hat{S}_z = \frac{\hbar}{2}\left(\hat{n}_\uparrow - \hat{n}_\downarrow\right) . \tag{2.65}$$

Expressing $\hat{S}^2$ is aided by knowing that,

$$\begin{aligned}
\hat{S}^2 &= \hat{S}_+\hat{S}_- + \hat{S}_z\left(\hat{S}_z - \hbar\hat{1}\right) \\
\hat{S}^2 &= \hat{S}_-\hat{S}_+ + \hat{S}_z\left(\hat{S}_z + \hbar\hat{1}\right) ,
\end{aligned} \tag{2.66}$$

which comes from the standard ladder operator treatment of angular momenta, and using the second-quantized forms of the raising and lowering operators,

$$\begin{aligned}
\hat{S}_+ &= \hbar\sum_r r^\dagger\bar{r} \\
\hat{S}_- &= \hbar\sum_r \bar{r}^\dagger r .
\end{aligned}$$

Then it is easy to derive that,

$$\hat{S}^2 = \hbar^2\hat{\mathcal{P}} + \frac{\hbar^2}{4}\left(\hat{n}_\uparrow - \hat{n}_\downarrow\right)^2 + \frac{\hbar^2}{2}\hat{n} , \tag{2.67}$$

where

$$\hat{n} = \hat{n}_\uparrow + \hat{n}_\downarrow \tag{2.68}$$

is the number operator which just counts the number of electrons in the wave function and

$$\hat{\mathcal{P}} = \sum_{r,s} r^\dagger\bar{s}^\dagger s\bar{r} \tag{2.69}$$

is the spin transposition operator which sums over all possible exchanges of $\alpha =\uparrow$ and $\beta =\downarrow$ pairwise exchanges.

We are now all set to apply these formulae to obtain our spin-adapted functions for the two-electron problem. The spin-coupling diagram (Fig. 2.4) tells us that there will be one one triplet ladder with $(S, M_S) = (1, +1), (1, 0), (1, -1)$ and one singlet ladder with $(S, M_S) = (0, 0)$. To find the head of the triplet ladder, we only need to identify the wave function with $M_S = 1$, namely

$$\Psi_{(1,+1)} = |\psi, \phi| . \tag{2.70}$$

We can verify that this is indeed a spin eigenfunction with the correct quantum numbers:

$$\begin{aligned}
\hat{S}_z\Psi_{(1,+1)} &= \frac{\hbar}{2}\left(\hat{n}_\uparrow - \hat{n}_\downarrow\right)|\psi, \phi| \\
&= \frac{\hbar}{2}(2-0)|\psi, \phi| \\
&= \hbar|\psi, \phi| \\
&\Rightarrow M_S = 1 \\
\hat{S}^2\Psi_{(1,+1)} &= \left(\hbar^2\hat{\mathcal{P}} + \frac{\hbar^2}{4}\left(\hat{n}_\uparrow - \hat{n}_\downarrow\right)^2 + \frac{\hbar^2}{2}\hat{n}\right)|\psi, \phi| \\
&= \left(0 + \frac{\hbar^2}{4}2^2 + \frac{\hbar^2}{2}2\right)|\psi, \phi| \\
&= 2\hbar^2|\psi, \phi| \\
&\Rightarrow S(S+1) = 2 \Rightarrow S = 1 .
\end{aligned} \tag{2.71}$$

Now we apply the spin lowering operator to find $\Psi_{(1,0)}$ by descending the ladder:

$$\begin{aligned}\hat{S}_-|\psi,\phi| &= \hbar\left(\sum_r \bar{r}^\dagger r\right)|\psi,\phi| \\ &= \hbar\left(|\bar{\psi},\phi| + |\psi,\bar{\phi}|\right) \\ &= \hbar\sqrt{2}\Psi_{(1,0)}\,, \end{aligned} \tag{2.72}$$

according to Eq. (2.58). Hence,

$$\Psi_{(1,0)} = \frac{1}{\sqrt{2}}\left(|\bar{\psi},\phi| + |\psi,\bar{\phi}|\right)\,, \tag{2.73}$$

but this result could just as easily be obtained by using the orthonormality of the determinants directly. Let us check that this is indeed a simultaneous eigenfunction of $\hat{S}_z$ and of $\hat{S}^2$:

$$\begin{aligned}\hat{S}_z\Psi_{(1,0)} &= \frac{\hbar}{2}\left(\hat{n}_\uparrow - \hat{n}_\downarrow\right)\frac{1}{\sqrt{2}}\left(|\bar{\psi},\phi| + |\psi,\bar{\phi}|\right) \\ &= \frac{\hbar}{2}(1-1)\frac{1}{\sqrt{2}}\left(|\bar{\psi},\phi| + |\psi,\bar{\phi}|\right) \\ &= 0\hbar\frac{1}{\sqrt{2}}\left(|\bar{\psi},\phi| + |\psi,\bar{\phi}|\right) \\ &\Rightarrow M_S = 0 \\ \hat{S}^2\Psi_{(1,0)} &= \left(\hbar^2\hat{\mathcal{P}} + \frac{\hbar^2}{4}\left(\hat{n}_\uparrow - \hat{n}_\downarrow\right)^2 + \frac{\hbar^2}{2}\hat{n}\right)\frac{1}{\sqrt{2}}\left(|\bar{\psi},\phi| + |\psi,\bar{\phi}|\right) \\ &= \hbar^2\left(1 + \frac{0}{4} + \frac{2}{2}\right)\frac{1}{\sqrt{2}}\left(|\bar{\psi},\phi| + |\psi,\bar{\phi}|\right) \\ &= 2\hbar^2\Psi_{(1,0)} = S(S+1)\hbar^2\Psi_{(1,0)} \\ &\Rightarrow S = 1\,. \end{aligned} \tag{2.74}$$

So it does check! To obtain $\Psi_{(1,-1)}$, apply the spin-lowering operator once again:

$$\hat{S}_-\Psi_{(1,-1)} = \hbar\left(\sum_r \bar{r}^\dagger r\right)\frac{1}{\sqrt{2}}\left(|\bar{\psi},\phi| + |\psi,\bar{\phi}|\right) = \sqrt{2}|\bar{\psi},\bar{\phi}|\,. \tag{2.75}$$

So, after normalization,

$$\Psi_{(1,-1)} = |\bar{\psi},\bar{\phi}|\,, \tag{2.76}$$

and we will leave it as an exercise to the reader to verify that this is a simultaneous eigenfunction of $\hat{S}_z$ and of $\hat{S}^2$ with the correct eigenvalues. We have missed $\Psi_{(0,0)}$ but we know it must be a linear combination of the two determinants with $M_S = 0$ — namely $|\bar{\psi},\phi|$ and $|\psi,\bar{\psi}|$ — and be orthogonal to $\Psi_{(1,0)}$. There is no choice left but

$$\Psi_{(0,0)} = \frac{1}{2}\left(|\bar{\psi},\phi| - |\psi,\bar{\phi}|\right)\,. \tag{2.77}$$

The reader is invited to verify that this is a simultaneous eigenfunction of $\hat{S}_z$ and of $\hat{S}^2$ with the correct eigenvalues and that both the raising and the lower operators annihilate $\Psi_{(0,0)}$. This confirms the main results of the previous subsection and provides some powerful tools for treating the case of more than $N = 2$ singly-occupied orbitals.

2.4.6 Ziegler-Rauk-Baerends Multiplet Sum Model

For all practical purposes, DFT is a SDET theory. However it is quite clear that the spin multiplets involve MDET wave functions. What to do? Ziegler, Rauk, and Baerends gave a clear answer pratical answer with their multiplet sum model (MSM) [59]. MSM

To be clear, this is not a formally justified method but rather a practical approach based upon reasonable physical intuition. Exact DFT applies only to (non-interacting v-representable) ground states and certainly not to excited states. Nevertheless it is common practice to assume that DFT may be used for the lowest state of each symmetry. This is really based upon the idea that all of the common density-functional approximations (DFAs) do a good job of describing *dynamical correlation* which is the residual electron correlation when a SDET wave function is a good first approximation. This is certainly the case for the $\Psi_{1,+1} = |g,u|$ state! Hence we may use this state in DFT to calculate the lowest triplet energy. But what about the corresponding open-shell singlet $\Psi_{0,0}$? For this, we need to use symmetry arguments to remove the zeroeth order degenerecy of our states. Correlation due to degeneracies (and hence associated with symmetry) is called *static correlation*. The MSM is based upon the observation that the singlet and triplet energies may be written as,

DFA, dynamical correlation

static correlation

$$
\begin{aligned}
E_T &= \langle g,u|\hat{H}|g,u\rangle = E[g,u] \\
E_T &= \frac{1}{2}\left(\langle g,\bar{u}| - \langle u,\bar{g}|\right)\hat{H}\left(|g,\bar{u}\rangle - |u,\bar{g}\rangle\right) \\
&= \langle g,\bar{u}|\hat{H}|g,\bar{u}\rangle - \langle g,\bar{u}|\hat{H}|u,\bar{g}\rangle \\
E_S &= \frac{1}{2}\left(\langle g,\bar{u}| - \langle u,\bar{g}|\right)\hat{H}\left(|g,\bar{u}\rangle + |u,\bar{g}\rangle\right) \\
&= \langle g,\bar{u}|\hat{H}|g,\bar{u}\rangle + \langle g,\bar{u}|\hat{H}|u,\bar{g}\rangle \,. \qquad (2.78)
\end{aligned}
$$

Hence, *assuming that the MOs used to construct the two states are the same*, we may calculate the triplet and open-shell singlet energies using only SDET energies,

$$
\begin{aligned}
E_S &= 2E_M - E_T \\
E_T &= \langle g,u|\hat{H}|g,u\rangle = E[g,u] \\
E_M &= \langle g,\bar{u}|\hat{H}|g,\bar{u}\rangle = E[g,\bar{u}] \,. \qquad (2.79)
\end{aligned}
$$

It is easy to construct the energy expressions for the TOTEM within wave function theory. I will use Mulliken charge cloud notation for electron repulsion integrals,

charge cloud notation, ERI

$$
[ik|jl] = \int \psi_i^*(1)\psi_k(1)\frac{1}{r_{1,2}}\psi_j^*(2)\psi_l(2)\, d1d2 \,, \qquad (2.80)
$$

which Szabo and Ostlund (page 68 of Ref. [60]) have popularized under the unfortunate name of "chemist's notation," though it seems to me that both chemists and physicists use this notation! In the deMon literature, we often use the alternative notation,

$$
(ik||jl) = [ik|jl] \,, \qquad (2.81)
$$

where the double bar ($||$) stands for $1/r_{1,2}$. I often use

$$
(ik|f_H|jl) = [ik|jl] \,, \qquad (2.82)
$$

where

$$
f_H(1,2) = \frac{\delta^2 E_H[\rho]}{\delta\rho(1)\delta\rho(2)} = \frac{1}{r_{1,2}} \,, \qquad (2.83)
$$

is the second functional derivative of the Hartree energy. This makes the notation easy to extend to the xc part of the DFT energy.

Ignoring DFT for the moment and keeping in mind that $[rr|ss]$ is a Coulomb repulsion integral between electrons regardless of their spin while $[rs|sr]$ is an exchange integral which arises only between electrons of the same spin, then the TOTEM energies are easily written as

$$\begin{aligned} E_T &= \epsilon_u^0 + \epsilon_g^0 + [gg|uu] - [gu|ug] \\ E_M &= \epsilon_u^0 + \epsilon_g^0 + [gg|uu] \,, \end{aligned} \tag{2.84}$$

so the multiplet splitting is just twice an exchange integral,

$$E_S - E_T = 2\,(E_M - E_T) = 2[gu|ug] > 0\,. \tag{2.85}$$

This is a consequence of the fact that the exchange integral acts to reduce the ERI between electrons of the same spin which avoid each other in space, thereby reducing their Coulomb repulsion. Of course, this splitting will go to zero if one orbital is very compact while the other is very diffuse, which is why we see that the multiplet splitting for Rydberg excitations is often negligeable.

Let us now turn to calculations with the MSM. For the initial calculations, we will ignore the condition that the same MOs should be used when calculating both E_T and E_M. Hence let us calculate them separately *allowing the MOs to relax in each case.* To calculate E_T, run

Contents of `H2triplet.inp`

```
TITLE H2 (Basis: SAD/GEN-A3*)
CHARGE 0
MULTI 3
#
SCFTYPE UKS
VXCTYPE VWN
#
PRINT MOS
#
# --- GEOMETRY ---
#
#
GEOMETRY CARTESIAN BOHR
H     0.000000    0.000000    0.000000
H     0.000000    0.000000    1.481211
#
AUXIS (GEN-A3*)
BASIS (SAD)
```

That was easy!

Optimizing the symmetry mixed-state is not quite so simple. To do this, we will first do the ground-state calculation:

Contents of `H2ground.inp`

```
TITLE H2 (Basis: SAD/GEN-A3*)
CHARGE 0
MULTI 1
#
SCFTYPE UKS
VXCTYPE VWN
#
PRINT MOS
#
# --- GEOMETRY ---
#
#
GEOMETRY CARTESIAN BOHR
H     0.000000    0.000000    0.000000
H     0.000000    0.000000    1.481211
#
AUXIS (GEN-A3*)
BASIS (SAD)
```

In principle, we could use the special MOMODIFY option of deMon2k to do a restart from this calculation and converge an SCF with different occupation numbers. However this is a tricky calculation which requires that the newly occupied MOs do not revert to the MOs occupied in the ground state. Unfortunately this is exactly what happens here if we try a straightforward strategy. MOMODIFY

Instead we will start from the ensemble average of the open-shell singlet and the three triplet states. This is the state with half an electron of each spin in σ_g and in σ_u.

Contents of H2ENS.inp

```
TITLE H2 ENS (Basis: SAD/GEN-A3*)
CHARGE 0
MULTI 1
#
SCFTYPE UKS
VXCTYPE VWN
MOMODIFY 2 2
1 0.5
2 0.5
1 0.5
2 0.5
#
PRINT MOS
#
# --- GEOMETRY ---
#
#
GEOMETRY CARTESIAN BOHR
H     0.000000    0.000000    0.000000
H     0.000000    0.000000    1.481211
```

```
#
AUXIS (GEN-A3*)
BASIS (SAD)
```

The `MOMODIFY` keyword modifies the MO occupation numbers to create the mixed symmetry state which is to be converged via an SCF procedure.

We may now proceed to change the occupation numbers and recalculate the new energies *without allowing any MO relaxation*. The key to this is to forbid any SCF iterations with the *MAX=0* keyword. To calculate the *unrelaxed* ground-state energy, we must start by making a copy of the restart (`.rst`) file that was created so that we may use it to optimize the mixed symmetry state. MAX=0 .rst

```
cp H2ENS.rst H2groundUNREL.rst
```

Then run

Contents of `H2groundUNREL.inp`

```
TITLE H2 ground unrelaxed (Basis: SAD/GEN-A3*)
CHARGE 0
MULTI 1
#
SCFTYPE UKS MAX=0
VXCTYPE VWN
GUESS RESTART
MOMODIFY 2 2
1 1.0
2 0.0
1 1.0
2 0.0
#
PRINT MOS
#
# --- GEOMETRY ---
#
#
GEOMETRY CARTESIAN BOHR
H     0.000000    0.000000    0.000000
H     0.000000    0.000000    1.481211
#
AUXIS (GEN-A3*)
BASIS (SAD)
```

The `GUESS RESTART` forces reading input information from `H2ENS.rst`. To calculate the *unrelaxed* triplet energy, GUESS RESTART

```
cp H2ENS.rst H2tripletUNREL.rst
```

Then run

Contents of `H2triplet.inp`

```
TITLE H2 triplet unrelaxed (Basis: SAD/GEN-A3*)
CHARGE 0
MULTI 1
#
SCFTYPE UKS MAX=0
VXCTYPE VWN
GUESS RESTART
MOMODIFY 2 2
1 1.0
2 1.0
1 0.0
2 0.0
#
PRINT MOS
#
# --- GEOMETRY ---
#
#
GEOMETRY CARTESIAN BOHR
H     0.000000    0.000000    0.000000
H     0.000000    0.000000    1.481211
#
AUXIS (GEN-A3*)
BASIS (SAD)
```

To calculate the *unrelaxed* mixed symmetry energy,

```
cp H2ENS.rst H2mixedUNREL.rst
```

Then run

Contents of `H2mixed.inp`

```
TITLE H2 mixed symmetry unrelaxed (Basis: SAD/GEN-A3*)
CHARGE 0
MULTI 1
#
SCFTYPE UKS MAX=0
VXCTYPE VWN
GUESS RESTART
MOMODIFY 2 2
1 1.0
2 0.0
1 0.0
2 1.0
#
PRINT MOS
#
# --- GEOMETRY ---
```

```
#
#
GEOMETRY CARTESIAN BOHR
H     0.000000    0.000000    0.000000
H     0.000000    0.000000    1.481211
#
AUXIS (GEN-A3*)
BASIS (SAD)
```

The MSM open-shell singlet energy is them calculated from $2E_M - E_T$.

1. Tabulate all the calculated total energies
2. Does the variational principle work?
3. What is the spin-multiplet splitting?
4. Do you notice anything else?

The MSM may also be applied in the case of spatial symmetry. We used this for O_2 in a remarkable collaboration which was only made possible because of people who met during ASESMA [61].

A final point worth thinking about is whether the MSM applies to delocalized orbitals in periodic calculations. In such a case, then changing orbital occupations does not lead to a significant change of the charge density, so energy differences just reduce to orbital energy differences which is going to cause the spin multiplet splitting to go (incorrectly) to zero. Hence the MSM is a molecular method and as system size grows (e.g., by growing silicon clusters), we should expect the quality of MSM calculations to gradually degrade.

2.4.7 Time-Dependent Density-Functional Theory

One of the main pragmatic problems with the MSM is that it is far from automatic. Orbitals need to be constructed for a multiplet ensemble and then several energies need to be calculated using different orbital occupations. In contrast, TD-DFT is a very automatic calculation thanks to the Casida equation. Casida equation

The Casida equation for TD-DFT was published in 1995 [62] and the first reported calculations were in 1996 [63, 64]. It is fair to claim priority because Reinhardt AHLRICHS, in a personal communication to me (MEC), explained that, although they had everything needed in their program to do TD-DFT calculations of excited states, it was not until reading Ref. [62] that they understood how such calculations could be justified. Since that time, there have been many variations on how to use TD-DFT to calculate absorption spectra and obtain information about excited states. These fall into two broad categories: (i) real-time calculations where the TD KS equation is propagated forward in real time and then the TD induced dipole moment is Fourier transformed to give an absorption spectrum and (ii) various variations and improvements on the implementation of the Casida equation. The idea behind the Casida equation was to cast TD-DFT in the form of what some chemists referred to as the random phase approximation (RPA). *Unfortunately the term RPA is frought with difficulty as it can mean very different things when calculating excitation energies or when calculating ground state correlation energies.* The term RPA was first introduced in nuclear physics. It was later applied to solids in periodic calculations where exchange diagrams were neglected. These diagrams are essential to keep for molecules and so some chemists, in an effort to avoid confusion, have used the RPA terms RPAE or RPAX to mean RPA *with exchange*. To make matters worse, RPA means something still different in the TD-DFT literature. So we will just keep the term Casida equations and avoid RPA except when it is used as a keyword in deMon2k.

As already mentioned, the first implementations of the Casida equation was in deMon2k [64] and in TurboMol [63]. In fact, many early advances in molecular methods and applications of DFT were first made by the deMon community. The solution of the Casida equation has continued to evolve and we will be using the version in the most recent (version 6.3) of deMon2k[65, 66]. As there is no manual for the new keywords needed to run these TD-DFT calculations, let us try to supply one here. Instead of the old `EXCITATION` keyword, we now have two new keywords:

Keyword CISTYPE
This keyword specifies what type of excited state calculation is to be done.
Options:
RPA / **TDA**

RPA Solve the Casida equation.

TDA Use the Tamm-Dancoff approximation.

Keyword CISDIA
This keyword specifies the CIS matrix diagonalization technique.
Options:
DAVIDSON / **RS** / **DSYEV** / **D&C** / **JACOB**I

DAVIDSON Iterative Davidson diagonalization of the TDDFT matrix. This is the default. It requires specifying **BAS** $= n$ where n is the maximum size of the Krylov space and **EIG** $= m$ which is the number of eigenvalues desired.

RS EISPACK Householder diagonalization of the TDDFT matrix. This is the default.

DSYEV LAPACK Householder diagonalization of the TDDFT matrix.

D&C LAPACK divide and conquer diagonalization of the TDDFT matrix.

JACOBI Jacobi diagonalization of the TDDFT matrix.

Description:
Excitation energies and oscillator strengths are calculated using the formulation of Ref. [64, 67, 68]. If full diagonalization is used, i.e., the option DAVIDSON is not used, then the oscillator strength sums are exact for the orbital basis set. In particular, this means that the dipole polarizability calculated as an oscillator strength sum is an analytic derivative value which should agree with the dipole polarizability found by the finite difference or other method. Note that if the Tamm-Dancoff approximation is used, the oscillator strength sums are no longer exact. The Tamm-Dancoff approximation [69, 70] can actually improve the quality of computed excitation energies when the molecular geometry is far from the equilibrium geometry.

One of the most important jobs of theory is to help experimentalists assign spectral transitions. From this point of view, it might be nice to have a simple absorption spectrum of H_2 and leave the assignment of the peaks as an exercise for the student. Unfortunately there are three problems with this. The first problem is that gas-phase H_2 is a simple enough molecule that high resolution absorption spectra are possible and detailed rovibrational absorption spectra have (understandably)

1 Ha	27.211399 eV	2 625.5002 kJ/mol	627.5096080305927 kcal/mol	
1 eV	0.03674930495120813 Ha	96.48530749925793 kJ/mol	23.060541945329334 kcal/mol	
1 kJ/mol	96.48530749925793 Ha	0.010364272330133138 eV	0.2390057361376673 kcal/mol	
1 kcal/mol	0.0015936010974213597 Ha	0.0433641153087705 eV	4.184 kJ/mol	
1 cm^{-1}	0.0000045563352812122295 Ha	0.0000045563352812122295 eV	0.011962659192089766 kJ/mol	0.0

Table 2.1: Some common units conversions obtained from the Colby energy converter. UV-Vis spectra are also often given in terms of wavelength. A handy formula converting energy E in eV to wavelength in nm is $\lambda = 1239.84193$ nm.eV$/E$.

been of greater interest in recent years (e.g., Ref. [71]) than have been measurements of electronic absorption spectra. The second problem is that the rovibrational lines in the absorption spectrum of H_2 strongly overlap, as shown in **Fig. 2.5**. And the final problem is that technology has changed. The older photographic film measurements of line spectra [72, 73] did not lend themselves to accurate intensity measurements. Instead, the student is asked to discover to what extent TD-DFT is able to calculate correctly the head (or close to the head) of the observed series: Lyman series, $X\,^1\Sigma_g \rightarrow B\,^1\Sigma_u$ at 95 160.3 cm^{-1} [73]; $X\,^1\Sigma_g \rightarrow E\,^1\Sigma_u$ bands at 110 815.65 cm^{-1} [73]; and the Werner bands $X\,^1\Sigma_g \rightarrow C\,^1\Pi_u$ at 99 409.18 cm^{-1} [73].

The issue of units also comes up again because different units are used by different people in different circumstances. There are several units converters on line. One that I like rather much is the Colby energy converter that you can find at:

`https://www.colby.edu/chemistry/PChem/Hartree.html`

Table 2.1 summarizes some key conversions.

Run

Contents of `H2full.inp`

```
TITLE H2 full TDDFT (Basis: SAD/GEN-A3*)
CHARGE 0
MULTI 1
#
SCFTYPE RKS
VXCTYPE VWN
#
# TD-ADFT CONTROLS
#
CISTYPE RPA
CISDIA BAS=100 EIG=10
#
PRINT MOS LCR
#
# --- GEOMETRY ---
#
#
GEOMETRY CARTESIAN BOHR
```

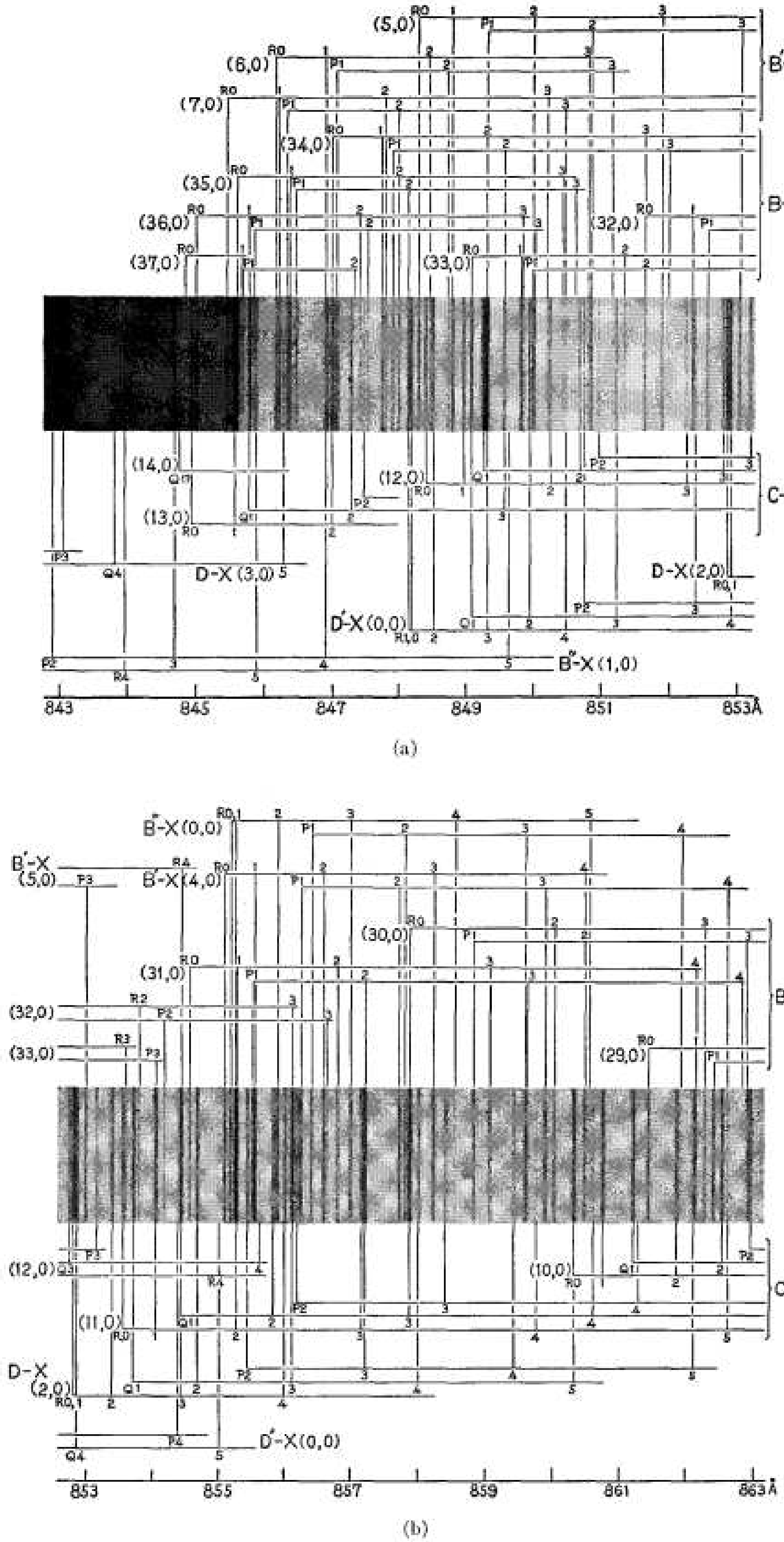

FIG. 1. (a) Absorption spectrum of the H_2 molecule in the wavelength region 843–853 Å. (b) Absorption spectrum of the H_2 molecule in the wavelength region 853–863 Å. In Fig. 1(a) the lines drawn to indicate the position of the $R(3)$ and $R(4)$ rotational lines of the D'–X (0, 0) band are incorrect. Those two rotational lines, $R(3)$ and $R(4)$, coincide in position with the C–X (12, 0) $Q(1)$ and the B–X (35, 0) $R(3)$, respectively.

Figure 2.5: H_2 experimental absorption spectrum from Ref. [72].

```
H     0.000000    0.000000    0.000000
H     0.000000    0.000000    1.481211
#
AUXIS (GEN-A3*)
BASIS (SAD)
```

Also carry out the calculation in the Tamm-Dancoff approximation (TDA). Run

Contents of `H2TDA.inp`

```
TITLE H2 full TDDFT (Basis: SAD/GEN-A3*)
CHARGE 0
MULTI 1
#
SCFTYPE RKS
VXCTYPE VWN
#
# TD-ADFT CONTROLS
#
CISTYPE TDA
CISDIA BAS=100 EIG=10
#
PRINT MOS LCR
#
# --- GEOMETRY ---
#
#
GEOMETRY CARTESIAN BOHR
H     0.000000    0.000000    0.000000
H     0.000000    0.000000    1.481211
#
AUXIS (GEN-A3*)
BASIS (SAD)
```

Note the important `LCR` option of `PRINT` stands for "local, charge-transfer, and Rydberg" and gives an MO analysis of the individual excitations.

1. The TD-DFT ionization threshold is at $-\epsilon_{\text{HOMO}}$. What is this in cm^{-1}?
2. Where are the TD-DFT iterations?
3. How could you check whether or not your TD-DFT calculations are converged with respect to the requested number of states?
4. Assign the spectrum.
5. Which transitions do you expect to have zero oscillator strengths?
6. What are the excitation energies in cm^{-1}?
7. Sketch the stick spectrum.

8. What is the spin multiplet splitting in Ha? How do the TD-DFT results compare with the results from the MSM?

9. Anything else?

2.5 Dissociation Limits

Ordinary DFAs have proven their worth for treating *dynamic correlation*. They fail to treat *static correlation* (i.e., correlation due to zero-order degeneracies). However the MSM is able to treat static correlation as is TD-DFT. This section concerns *nondynamic correlation* due to *quasi*degeneracies. These arise frequently between states whose zero-order approximations approach in energy near certain geometries—frequently exactly where bonds are being made or broken. Hence the ability to treat nondynamic correlation should be critical when studying chemical reaction paths. It turns out that TD-DFT is sensitive to the failure of TD-DFT to properly incorporate nondynamic correlation in the ground state and so may be used to understand where DFAs fail in ground state calculations.

2.5.1 Valence-Bond Picture

This subsection is taken nearly verbatim from Workbook 1 [1, 2].

One (overly narrow) definition of chemistry is that it is all about chemical reactions, i.e., making and breaking bonds. The dissociation

$$\mathrm{H}_2 \rightarrow 2\mathrm{H}\,, \tag{2.86}$$

has two possible products, namely ions (homolytic bond cleavage),

$$\left[\mathrm{H}\!:^- + \mathrm{H}^+ \leftrightarrow \mathrm{H}^+ + \mathrm{H}\!:^-\right]\,, \tag{2.87}$$

and radicals (heterolytic bond cleavage),

$$\left[\mathrm{H}^\uparrow + \mathrm{H}^\downarrow \leftrightarrow \mathrm{H}^\downarrow + \mathrm{H}^\uparrow\right]\,. \tag{2.88}$$

Note that thermal (i.e., ground-state) dissociation corresponds to dissociation into radicals. Other heterolytic outcomes are,

$$\mathrm{H}^\uparrow + \mathrm{H}^\uparrow\,, \tag{2.89}$$

and,

$$\mathrm{H}^\downarrow + \mathrm{H}^\downarrow\,, \tag{2.90}$$

Let us check the dissociation limits of our wave functions. To do so, we must re-express our wave functions in terms of atomic orbitals and then follow the old valence-bond practice [74] of associating wave functions with Lewis dot structures [4].

In the limit of $R = \infty$, then $S = 0$ and our orbitals become

$$\begin{aligned}
\sigma_g &= \frac{1}{\sqrt{2}}(s_A + s_B) \\
\sigma_u &= \frac{1}{\sqrt{2}}(s_A - s_B)\,,
\end{aligned} \tag{2.91}$$

In this same limit,

$$\begin{aligned}
\Psi_{(1,1)} &= |\sigma_g, \sigma_u| \\
&= \frac{1}{2}|s_A + s_B, s_A - s_B| \\
&= \frac{1}{2}\left(-|s_A, s_B| + |s_B, s_A|\right) \\
&= -|s_A, s_B| \,, \qquad (2.92)
\end{aligned}$$

which corresponds to the Lewis dot structure (2.89). Similarly,

$$\Psi_{(1,-1)} = |\bar{\sigma}_g, \bar{\sigma}_u| = -|\bar{s}_A, \bar{s}_B| \,, \qquad (2.93)$$

which corresponds to the Lewis dot structure (2.90). We might expect that the dissociation limit of $\Psi_{(1,0)}$ is given by the Lewis dot structure (2.88) and this indeed is true:

$$\begin{aligned}
\Psi_{(1,0)} &= \frac{1}{\sqrt{2}}\left(|\sigma_u, \bar{\sigma}_g| - |\sigma_g, \bar{\sigma}_u|\right) \\
&= \frac{1}{2\sqrt{2}}\left(|s_A - s_B, \bar{s}_A + \bar{s}_B| - |s_A + s_B, \bar{s}_A - \bar{s}_B|\right) \\
&= \frac{1}{2\sqrt{2}}\left[\left(|s_A, \bar{s}_A| + |s_A, \bar{s}_B| - |s_B, \bar{s}_A| - |s_B, \bar{s}_B|\right) - \left(|s_A, \bar{s}_A| - |s_A, \bar{s}_B| + |s_B, \bar{s}_A| - |s_B, \bar{s}_B|\right)\right] \\
&= \frac{1}{\sqrt{2}}\left(|s_A, \bar{s}_B| - |s_B, \bar{s}_A|\right) \,. \qquad (2.94)
\end{aligned}$$

We now come to the famous problem of the dissociation of the ground-state wave function. According to naïve MO theory, the ground-state wave function is,

$$\begin{aligned}
\Psi^1_{(0,0)} &= |\sigma_g, \bar{\sigma}_g| \\
&= \frac{1}{2}|s_A + s_B, \bar{s}_A + \bar{s}_B| \\
&= \frac{1}{2}\left(|s_A, \bar{s}_A| + |s_B, \bar{s}_B|\right) + \frac{1}{2}\left(|s_A, \bar{s}_B| + |s_B, \bar{s}_A|\right) \,. \qquad (2.95)
\end{aligned}$$

That is,

$$\Psi^1_{(0,0)} = \frac{1}{\sqrt{2}}\left(\Psi^{\text{ionic}}_{(0,0)} + \Psi^{\text{covalent}}_{(0,0)}\right) \,, \qquad (2.96)$$

is an equal mixture of a covalent wave function,

$$\Psi^{\text{covalent}}_{(0,0)} = \frac{1}{\sqrt{2}}\left(|s_A, \bar{s}_B| + |s_B, \bar{s}_A|\right) \,, \qquad (2.97)$$

corresponding to the expected dissociation into radicals [Lewis dot structure (2.88)] and an ionic wave function,

$$\Psi^{\text{ionic}}_{(0,0)} = \frac{1}{\sqrt{2}}\left(|s_A, \bar{s}_A| + |s_B, \bar{s}_B|\right) \,, \qquad (2.98)$$

corresponding to dissociation into ions [Lewis dot structure (2.87)]. The presence of the ionic term means that MO theory will not dissociate correctly, but rather will dissociate to too high an energy.

In order to correct the problem, let us look at the $R \to \infty$ limit of the doubly-excited determinant,

$$\begin{aligned}
\Psi^2_{(0,0)} &= |\sigma_u, \bar{\sigma}_u| \\
&= \frac{1}{2}|s_A - s_B, \bar{s}_A - \bar{s}_B| \\
&= \frac{1}{2}\left(|s_A, \bar{s}_A| + |s_B, \bar{s}_B|\right) - \frac{1}{2}\left(|s_A, \bar{s}_B| + |s_B, \bar{s}_A|\right) \\
&= \frac{1}{\sqrt{2}}\left(\Psi^{\text{ionic}}_{(0,0)} - \Psi^{\text{covalent}}_{(0,0)}\right) . \qquad (2.99)
\end{aligned}$$

Apparently the correct dissociation limit requires the linear combination,

$$\frac{1}{\sqrt{2}}\left(\Psi^1_{(0,0)} - \Psi^2_{(0,0)}\right) = \Psi^{\text{covalent}}_{(0,0)} , \qquad (2.100)$$

as $R \to 0$. Note that ${}^{(0,0)}\Psi_{\text{covalent}}$ is the Heitler-London [valence-bond (VB)] wave function,

$$\Psi^{\text{covalent}}_{(0,0)} = \left[\frac{1}{\sqrt{2}}\left(s_A(1)s_B(2) + s_B(1)s_A(2)\right)\right]\left[\frac{1}{2}\left(\alpha(1)\beta(2) - \beta(1)\alpha(2)\right)\right] . \qquad (2.101)$$

As neither the naïve MO wave function nor the naïve VB wave function are correct at all R, but the MO wave function is best near the equilibrium geometry and the VB wave function is best near dissociation, then the recommended choice is to take a linear combination,

$$\begin{aligned}
\Psi_{(0,0)} &= C_1\Psi^1_{(0,0)} - C_2\Psi^2_{(0,0)} \\
&= C_{\text{ionic}}\Psi^{\text{ionic}}_{(0,0)} + C_{\text{covalent}}\Psi^{\text{covalent}}_{(0,0)} , \qquad (2.102)
\end{aligned}$$

with R-dependent coefficients whose values should be determined variationally. Equation (2.102) is an example of a configuration-interaction (CI) wave function. CI wave functions are often necessary for describing chemical reactions because, by taking a geometry-dependent linear combination of the product and reactant wave functions, the CI wave function provides a smooth interpolation along the chemical reaction pathway.

The EXACT PECs relevant for the σ_g+σ_u TOTEM are

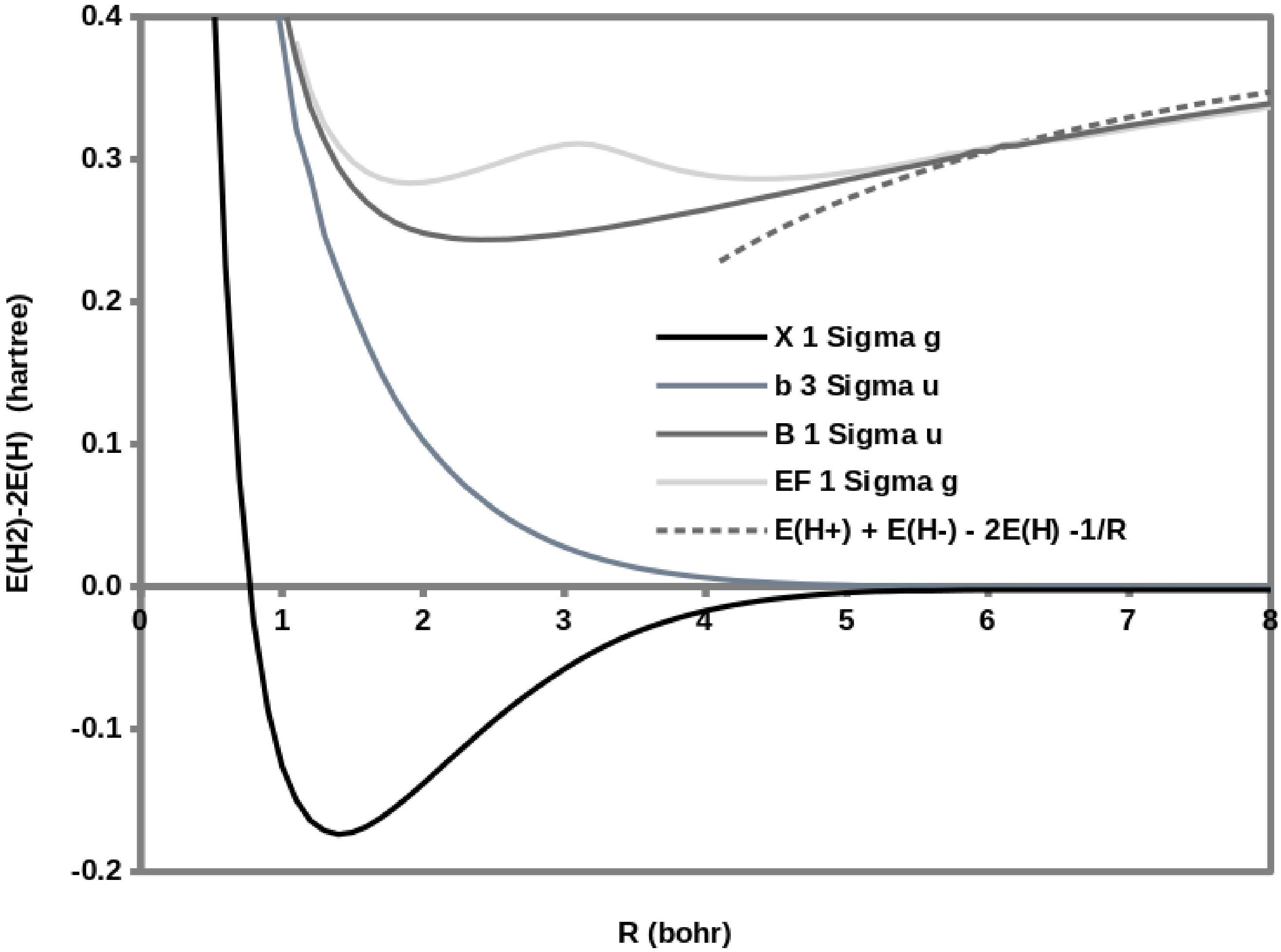

Notice how the different states either dissociate to [H· ·H] at large bond distance or dissociate to [H^+ :H^- ↔ H:$^-$ H^+] as predicted by VB theory.

2.5.2 TD-DFT and Symmetry Breaking

Let us do something very simple—namely, let us repeat the full TD-DFT calculations at a variety of bond distances. This is best done by dividing up the work into, say, 3 working groups of students.

Group 1 will carry out TD-DFT calculations for the bond lengths R = 1.1 bohr, 1.2 bohr, ..., 3.0 bohr.

Group 2 will carry out TD-DFT calculations for the bond lengths R = 3.1 bohr, 3.2 bohr, ..., 5.0 bohr.

Group 3 will carry out TD-DFT calculations for the bond lengths R = 5.1 bohr, 5.2 bohr, ..., 6.9 bohr.

This means running

```
TITLE H2 full TDDFT (Basis: SAD/GEN-A3*)
CHARGE 0
MULTI 1
```

```
#
SCFTYPE RKS
VXCTYPE VWN
#
# TD-ADFT CONTROLS
#
CISTYPE RPA
CISDIA BAS=100 EIG=30
#
PRINT MOS LCR
#
# --- GEOMETRY ---
#
#
GEOMETRY CARTESIAN BOHR
H     0.000000    0.000000    0.000000
H     0.000000    0.000000    x.xxxxxx
#
AUXIS (GEN-A3*)
BASIS (SAD)
```

for different bond lengths x.xxxxxx. We will collect the results and compare them against the tabulated EXACT values from Sec. 1.4 for the $X\,^1\Sigma_g$, $b\,^3\Sigma_u$, and $B\,^1\Sigma_u$ states. Note that a "negative" excitation energy is really a way of representing an *imaginary* excitation energy in the case of a full TD-DFT calculation. This is an indication that something is wrong with the ground state because it is responding incorrectly to an applied electric field. *What can you conclude from the computational results?*

What we are seeing is a problem due to the lack of nondynamical (i.e., quasidegenerate) correlation in DFT. One way to address this problem with the ground state is to do spin-unrestricted KS (UKS) calculations that allow different-orbitals-for-different-spins (DODS). A problem with such calculations is that the initial guess has the same-orbitals-for-different-spins (SODS) and it can be difficult to make DFT programs break orbital symmetry during the SCF iterations. So, we will use a trick: We will first carry out a triplet calculation. Run UKS, DODS, SODS

```
TITLE H2 Symmetry Breaking (Basis: SAD/GEN-A3*)
CHARGE 0
MULTI 3
#
SCFTYPE UKS
VXCTYPE VWN
#
PRINT MOS
#
# --- GEOMETRY ---
#
#
GEOMETRY CARTESIAN BOHR
H     0.000000    0.000000    0.000000
```

```
H     0.000000    0.000000    x.xxxxxx
#
AUXIS (GEN-A3*)
BASIS (SAD)
```

which will typically give DODS. Now use the restart file for the UKS singlet. That is, run

```
TITLE H2 Symmetry Breaking (Basis: SAD/GEN-A3*)
CHARGE 0
MULTI 1
#
SCFTYPE UKS
VXCTYPE VWN
GUESS RESTART
#
PRINT MOS
#
# --- GEOMETRY ---
#
#
GEOMETRY CARTESIAN BOHR
H     0.000000    0.000000    0.000000
H     0.000000    0.000000    x.xxxxxx
#
AUXIS (GEN-A3*)
BASIS (SAD)
```

Once you have converged broken symmetry `MULTI 1` calculations at longer bond lengths, then you can use the `.rst` file for geometries with shorter bond lengths. Keep doing this, noting down the spin contamination $\langle \hat{S}^2 \rangle$ as you go. Graph the PEC and also $\langle \hat{S}^2 \rangle$ as a function of bond length. Let us try to divide up the work among the three groups! *Now what do you conclude?*

If time allows, repeat the calculation of PECs using the TDA. Remember that a negative excitation energy in a TDA calculation is really a real excitation energy that is negative!

```
TITLE H2 TDA TDDFT (Basis: SAD/GEN-A3*)
CHARGE 0
MULTI 1
#
SCFTYPE RKS
VXCTYPE VWN
#
# TD-ADFT CONTROLS
#
CISTYPE TDA
CISDIA BAS=100 EIG=30
#
PRINT MOS LCR
#
# --- GEOMETRY ---
```

```
#
#
GEOMETRY CARTESIAN BOHR
H     0.000000    0.000000    0.000000
H     0.000000    0.000000    x.xxxxxx
#
AUXIS (GEN-A3*)
BASIS (SAD)
```

Now what can we conclude?

2.5.3 Diagrammatic MSM

Symmetry breaking is one way to include some nondynamic correlation in DFT calculations. It seems appropriate to mention another attempt precisely because it developed out of an ASESMA project. This is the use of a diagrammatic analysis of CI matrix elements which allows reasonable guesses as to the form of DFT matrix elements in a simple model for including nondynamic correlation in DFT [75, 76]:

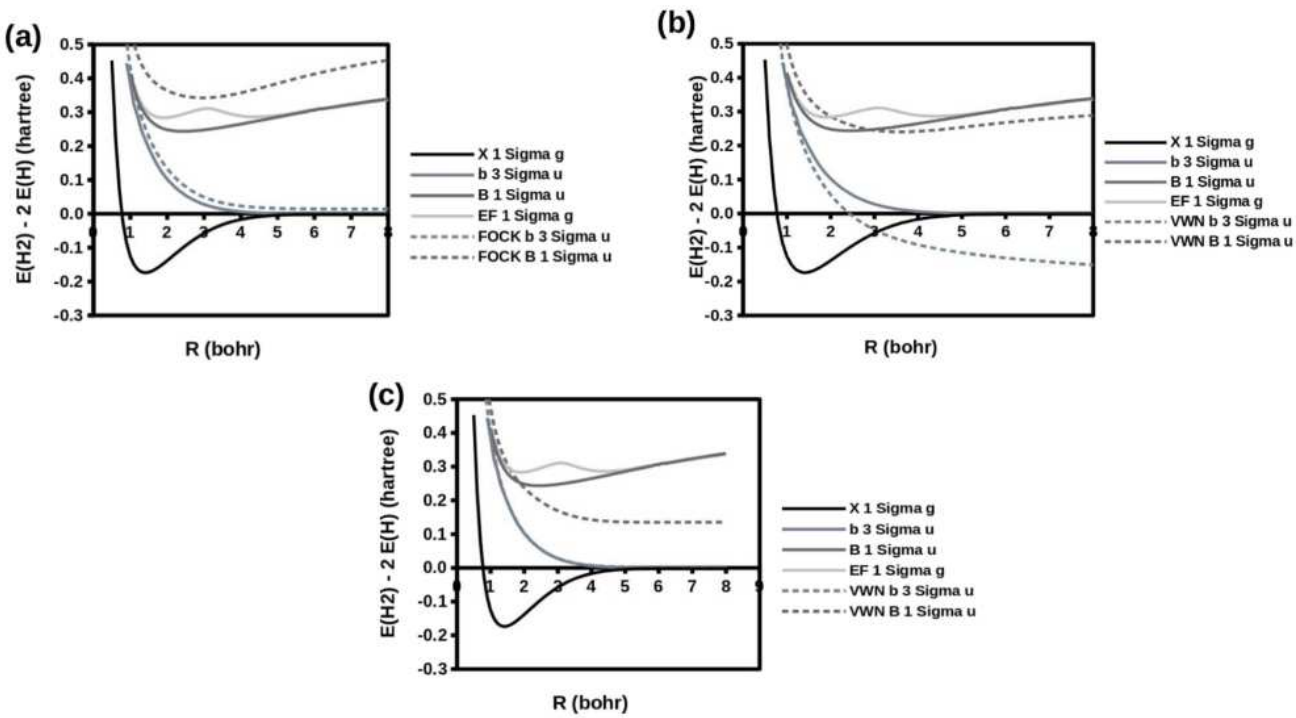

FIG. 14. Three ways to calculate MSM $b\ ^3\Sigma_u$ and $B\ ^1\Sigma_u$ PECs: (a) MSM-HF, (b) MSM-VWN using HF A, and (c) MSM-VWN (using VWN A).

It involves several interesting new ideas, some of which work better than others. Though the theory is imperfect, it is still evolving and I have no doubt that it can be much improved.

Chapter 3

Answers

3.1 Answers for Section 2.4

3.1.1 Bond Dissociation Energy

The Sadlej basis set for H consists of 3 s-type GTOs and 2 sets of p-type GTOs. As each set of p-type GTOs is composed of three functions (p_x, p_y, and p_z) then the total number of AOs in the Sadlej basis set consists of $3 + 2 \times 3 = 9$ AOs. This is evident in the output files for the calculations of H^+, H, and H^-.

H^+ consists of a single positively charged nucleus and no electrons. Its energy is rigorously 0.0 Ha.

The Schrödinger equation for the H atom may be solved analytically and $E(\mathrm{H})$ = -0.5 Ha *exactly*. Of course, we do not get this with our finite basis sets and especially we do not get the exact answer because the LDA is not exact. Instead we get $E(\mathrm{H})$ = -0.478497984 Ha at the LDA/SAD/GEN-A3* level. The spin α MO coefficients are:

				1	2	3	4	5
				-0.2687	0.0318	0.1010	0.1010	0.1010
				1.0000	0.0000	0.0000	0.0000	0.0000
1	1	H	1s	0.6570	-0.2594	0.0000	0.0000	0.0000
2	1	H	2s	0.3907	-0.6886	0.0000	0.0000	0.0000
3	1	H	3s	0.0477	1.4265	0.0000	0.0000	0.0000
4	1	H	2py	0.0000	-0.0000	0.0000	0.0120	0.0000
5	1	H	2pz	0.0000	-0.0000	0.0000	0.0000	0.0120
6	1	H	2px	0.0000	-0.0000	0.0120	0.0000	0.0000
7	1	H	3py	0.0000	-0.0000	0.0000	0.9925	0.0000
8	1	H	3pz	0.0000	-0.0000	0.0000	0.0000	0.9925
9	1	H	3px	0.0000	-0.0000	0.9925	0.0000	0.0000

				6	7	8	9
				0.4346	0.7971	0.7971	0.7971
				0.0000	0.0000	0.0000	0.0000

```
   1   1   H   1s      -1.3684   -0.0000   -0.0000   -0.0000
   2   1   H   2s       2.1851   -0.0000   -0.0000   -0.0000
   3   1   H   3s      -1.0715   -0.0000   -0.0000   -0.0000
   4   1   H   2py      0.0000    1.2774   -0.0000   -0.0000
   5   1   H   2pz      0.0000   -0.0000   -0.0000    1.2774
   6   1   H   2px      0.0000   -0.0000    1.2774   -0.0000
   7   1   H   3py      0.0000   -0.8043   -0.0000   -0.0000
   8   1   H   3pz      0.0000   -0.0000   -0.0000   -0.8043
   9   1   H   3px      0.0000   -0.0000   -0.8043   -0.0000
```

MO 1 is a nodeless $1s$ AO, MO 2 is a $2s$ AO with a radial node, MOs 3-5 are $2p$ AOs, MO 6 is a $3s$ AO with two radial nodes, MOs 7-9 are $3p$ AOs with one radial node. Note though that the unoccupied AOs are unlikely to be very exact. Notice also that the energy of the $1s$ AO is $\epsilon_{1s} =$ -0.2689 Ha, which is considerably larger than the exact $E(\mathrm{H}) =$ -0.5 Ha. Underbinding of electrons is typical of DFT because the xc-potential goes to zero to quickly at large distance from the nucleus. The spin β MO coefficients are:

```
BETA MO COEFFICIENTS OF CYCLE 6


                            1         2         3         4         5
                      -0.0998    0.0648    0.1441    0.1441    0.1441

                       0.0000    0.0000    0.0000    0.0000    0.0000

   1   1   H   1s       0.3904   -0.2370    0.0000    0.0000    0.0000
   2   1   H   2s       0.4241   -1.0656    0.0000    0.0000    0.0000
   3   1   H   3s       0.3355    1.4932    0.0000    0.0000    0.0000
   4   1   H   2py      0.0000   -0.0000    0.0000    0.0000   -0.0638
   5   1   H   2pz      0.0000   -0.0000   -0.0638    0.0000    0.0000
   6   1   H   2px      0.0000   -0.0000    0.0000   -0.0638    0.0000
   7   1   H   3py      0.0000   -0.0000    0.0000    0.0000    1.0385
   8   1   H   3pz      0.0000   -0.0000    1.0385    0.0000    0.0000
   9   1   H   3px      0.0000   -0.0000    0.0000    1.0385    0.0000

                            6         7         8         9
                       0.5919    0.9529    0.9529    0.9529

                       0.0000    0.0000    0.0000    0.0000

   1   1   H   1s      -1.4707   -0.0000   -0.0000   -0.0000
   2   1   H   2s       2.0214   -0.0000   -0.0000   -0.0000
   3   1   H   3s      -0.9182   -0.0000   -0.0000   -0.0000
   4   1   H   2py      0.0000   -0.0000    1.2759   -0.0000
   5   1   H   2pz      0.0000   -0.0000   -0.0000    1.2759
   6   1   H   2px      0.0000    1.2759   -0.0000   -0.0000
   7   1   H   3py      0.0000   -0.0000   -0.7440   -0.0000
   8   1   H   3pz      0.0000   -0.0000   -0.0000   -0.7440
```

```
    9    1   H    3px         0.0000     -0.7440     -0.0000     -0.0000
```

Corresponding α and β MOs typically have different energies in spin-unrestricted calculations.

According to the Wikipedia entry for the "Hydrogen anion," the electron affinity (EA) of the hydrogen atom is 0.027716 Ha. As EA

$$E(\mathrm{H}^-) = E(\mathrm{H}) - \mathrm{EA} = \text{-}0.527716 \text{ Ha}. \tag{3.1}$$

Hence we can calculate the LDA/SAD/GEN-A3* energy. First makes sure that you find the `CONVERGED` keyword in the output file! In this case, the calculation has converged. The LDA/SAD/GEN-A3* value is $E(\mathrm{H}^-) =$ -0.51106 Ha. The spin α and β $1s$ orbital energies are the same $\epsilon_{1s} = 0.0655$ Ha. As this is a positive energy, the electron is not even bound. Strictly speaking, *such a calculation cannot be converged with respect to the quality of the orbital basis set and so should be discarded.* However this is just an exercise, so we shall keep it.

The EXACT bond length of H_2 is $R_e = 1.4$ bohr. The corresponding bond energy is $D_e = 0.1740$ Ha. The optimization of H_2 started out with a very bad guess for the H_2 bond length. 18 self-consistent field (SCF) calculations had to be converged. Each time forces were calculated and the atoms were moved to minimize the energy until the gradient of the energy was considered small enough for a geometry optimization convergence. We see SCF

```
 *** CONVERGED BY GRADIENT AND DISPLACEMENT CRITERIA ***
 *** AFTER 17 OPTIMIZATION CYCLES ***


 RMSQ FORCE :   0.0000003  MAXIMUM :   0.0003000  CONVERGED :YES
 MAX FORCE  :   0.0000003  MAXIMUM :   0.0004500  CONVERGED :YES
 RMSQ DR    :   0.0002969  MAXIMUM :   0.0012000  CONVERGED :YES
 MAX DR     :   0.0002969  MAXIMUM :   0.0018000  CONVERGED :YES
```

Once converged, we find

```
*** OPTIMIZED Z-MATRIX VARIABLES IN BOHR ***

 R1              1.481211


 FINAL INPUT ORIENTATION IN BOHR

  NO.  ATOM        X              Y              Z        Z-ATOM   MASS   TYPE

    1  H         0.000000       0.000000       0.000000       1      1.008  QM
    2  H         0.000000       0.000000       1.481211       1      1.008  QM
```

We see that the LDA/SAD/AUG-A3* bond distance is $R_e = 1.481211$ bohr. The corresponding bond dissociation energy is

$$D_e = 2E(\mathrm{H}) = E(\mathrm{H}_2) = 2\,(\text{-}0.478497984 \text{ Ha}) - (\text{-}1.133460233 \text{ Ha}) = 0.1764642 \text{ Ha}. \tag{3.2}$$

The LDA is known to overbind molecules. In this case, the overbinding is by 0.025 Ha or 16 kcal/mol. This is much too large for accurate chemical calculations. The ideal chemical accuracy chemical accuracy (i.e., the accuracy of thermodynamic bond energy measurements on small molecules) is 1 kcal/mol 0.001594 Ha.

Here are my sketches of the first nine MOs based upon their coefficients:

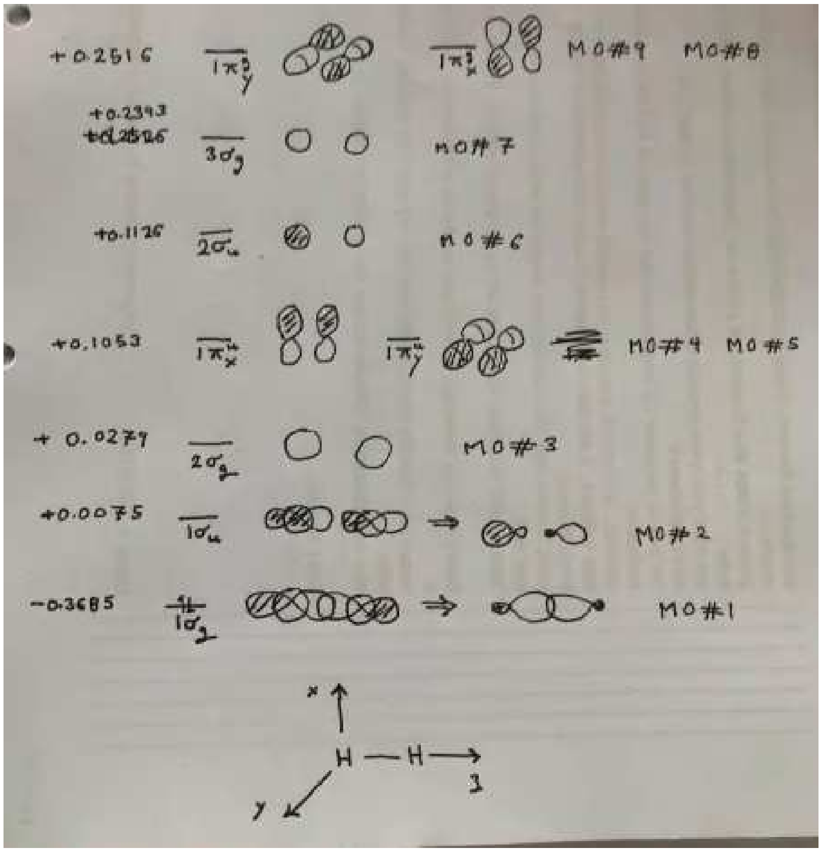

Note that software such as Molden [77, 78, 79] may be used to visualize MOs produced by deMon2k. However it is a valuable learning step to be able to read MO coefficients and visualize from them what the MOs look like in the case of simple molecules. Molden

3.1.2 Excitation Energies

MSM

State	Relaxed Energy	Unrelaxed Energy
ENS	—	-0.703224291
S	—	-0.692537600
M	—	-0.731688919
T	-0.773127251	-0.770840238
GS	-1.131900722	-1.118587678

The unrelaxed ground state (GS) energy is above the relaxed GS energy as it should be. Similarly the unrelaxed triplet energy is above the relaxed triplet energy as dictated by the variational principle. The MSM spin multiplet spitting $E_S - E_T = 0.07830$ Ha which may be compared with the EXACT value of 0.07421 Ha. GS

TD-DFT The TD-DFT converged in three iterations:

```
   DAVIDSON DIAGONALIZATION
  ITER    CONV    VECT        RMS

   1      19      30      9.486748
   2      19      11      6.944118
   3      30      15      6.031923
 ------------------------------------------------
 COMMENT : EQUAL NUMBER OF S AND T STATES     15      15
 ------------------------------------------------
```

The Davidson method only calculates the lowest energy part of the spectrum. You have to keep requesting more states until this part of your calculated spectrum has stabilized. Otherwise it is not converged. Another thing to know about the Davidson method is that it may miss excitation energies. As a general rule of thumb (ROT), you should ask for double the number of excitation energies than you actually want, just to insure that the values you really want are actually found. ROT

Oscillator strengths (i.e., the intensity of line spectra) are determined by transition dipole moment $|\langle I|\vec{r}|J\rangle$
$vert^2$ selection rules. Notice that this does not involve spin (photons do not carry spin that they can transfer to electrons!) That means that singlet → triplet oscillator strengths will also be zero. Furthermore, $\Sigma_g \rightarrow \Sigma_g$ transitions are also forbidden by symmetry.

One of the problems is how to assign the excited states. You have already drawn cartoons of the MOs. So let us just list them here:

MO	label
1	$1\sigma_g$
2	$1\sigma_u$
3	$2\sigma_g$
4 & 5	$1\pi_u$
6	$2\sigma_u$
7	$3\sigma_g$
8 & 9	$1\pi_g$

Let us take a look at the assignment problem for the triplets first. Here are results from the full TD-DFT calculation:

```
 +==================================+
   1    9.4650 eV T LAMBDA: 0.52    3Sigma_u
 +-----------ALPHA-ALPHA-----------+
                   [eV]      COEFF
    1 -->    2   10.2147  -0.9725  1sigma_g -> 1sigma_u
    1 -->    6   13.0747  -0.2244  1sigma_g -> 2sigma_u
 +==================================+
   3   10.5276 eV T LAMBDA: 0.34     3Sigma_g
 +-----------ALPHA-ALPHA-----------+
```

```
                  [eV]     COEFF
    1 -->    3   10.7754  -0.9987   1sigma_g -> 2sigma_g
+==================================+
  5   12.2438 eV T LAMBDA: 0.51     3Pi_u
+-----------ALPHA-ALPHA-----------+
                  [eV]     COEFF
    1 -->    4   12.8812  -0.9876   1sigma_g -> 1pi_u
    1 -->    5   12.8812  -0.1529   1sigma_g -> 1pi_u
+==================================+
  6   12.2438 eV T LAMBDA: 0.51     3Pi_u
+-----------ALPHA-ALPHA-----------+
                  [eV]     COEFF
    1 -->    4   12.8812   0.1529   1sigma_g -> 1pi_u
    1 -->    5   12.8812  -0.9876   1sigma_g -> 1pi_u
+==================================+
  7   12.4206 eV T LAMBDA: 0.55     3Sigma_u
+-----------ALPHA-ALPHA-----------+
                  [eV]     COEFF
    1 -->    2   10.2147   0.2287   1sigma_g -> 1sigma_u
    1 -->    6   13.0747  -0.9706   1sigma_g -> 2sigma_u
    1 -->   10   19.9156  -0.0617   1sigma_g -> ???
+==================================+
 13   16.1178 eV T LAMBDA: 0.42     3Sigma_g
+-----------ALPHA-ALPHA-----------+
                  [eV]     COEFF
    1 -->    7   16.5290  -0.9978   1sigma_g -> 3sigma_g
    1 -->   11   21.1435   0.0550   1sigma_g -> ???
+==================================+
15   16.5156 eV T LAMBDA: 0.32      3Pi_g
+-----------ALPHA-ALPHA-----------+
                  [eV]     COEFF
    1 -->    8   16.8567   0.8181   1sigma_g -> 1pi_g
    1 -->    9   16.8568  -0.5750   1sigma_g -> 1pi_g
+==================================+
 16   16.5156 eV T LAMBDA: 0.32     3Pi_g
+-----------ALPHA-ALPHA-----------+
                  [eV]     COEFF
    1 -->    8   16.8567  -0.5750   1sigma_g -> 1pi_g
    1 -->    9   16.8568  -0.8181   1sigma_g -> 1pi_g
+==================================+
 17   19.3361 eV T LAMBDA: 0.51     3Sigma_u
+-----------ALPHA-ALPHA-----------+
                  [eV]     COEFF
    1 -->    6   13.0747  -0.0752   1sigma_g -> 2sigma_u
    1 -->   10   19.9156   0.9933   1sigma_g -> ???
    1 -->   12   27.0528   0.0790   1sigma_g -> ???
+==================================+
```

```
 18   20.0331 eV T LAMBDA: 0.67     3Sigma_g
+-----------ALPHA-ALPHA-----------+
                  [eV]     COEFF
   1 -->    7   16.5290  -0.0563   1sigma_g -> 3sigma_g
   1 -->   11   21.1435  -0.9978   1sigma_g -> ???
+=================================+
 21   25.8496 eV T LAMBDA: 0.64
+-----------ALPHA-ALPHA-----------+
                  [eV]     COEFF
   1 -->   10   19.9156   0.0835
   1 -->   12   27.0528  -0.9952
+=================================+
 22   27.9004 eV T LAMBDA: 0.77
+-----------ALPHA-ALPHA-----------+
                  [eV]     COEFF
   1 -->   13   29.5513  -0.9993
+=================================+
 23   27.9004 eV T LAMBDA: 0.77
+-----------ALPHA-ALPHA-----------+
                  [eV]     COEFF
   1 -->   14   29.5513  -0.9993
+=================================+
 27   39.9933 eV T LAMBDA: 0.80
+-----------ALPHA-ALPHA-----------+
                  [eV]     COEFF
   1 -->   15   41.8200  -0.9999
+=================================+
 28   41.3383 eV T LAMBDA: 0.73
+-----------ALPHA-ALPHA-----------+
                  [eV]     COEFF
   1 -->   16   42.9749  -0.9999
+=================================+
```

Now let us do the same thing for the singlets.

```
+=================================+
  2   10.5104 eV S LAMBDA: 0.53     1Sigma_u
+-----------ALPHA-ALPHA-----------+ S=0.2138
                  [eV]     COEFF
   1 -->    2   10.2147  -0.9681   1sigma_g -> 1sigma_u
   1 -->    6   13.0747   0.2386   1sigma_g -> 2sigma_u
   1 -->   10   19.9156   0.0573   1sigma_g -> ????
   1 -->   12   27.0528   0.0504
+=================================+
  4   10.9373 eV S LAMBDA: 0.34     1Sigma_u
+-----------ALPHA-ALPHA-----------+ S=0.0000
                  [eV]     COEFF
   1 -->    3   10.7754   0.9967   1sigma_g -> 1sigma_u
```

```
   1 -->   11   21.1435  -0.0684   1sigma_g -> ???
+==================================+
  8   12.8186 eV S LAMBDA: 0.51     1Pi_u
+-----------ALPHA-ALPHA-----------+ S=0.3534
                  [eV]      COEFF
   1 -->    5   12.8812   0.9980   1sigma_g -> 1pi_u
   1 -->   14   29.5513   0.0520   1sigma_g -> ???
+==================================+
  9   12.8195 eV S LAMBDA: 0.51     1Pi_u
+-----------ALPHA-ALPHA-----------+ S=0.3534
                  [eV]      COEFF
   1 -->    4   12.8812   0.9980   1sigma_g -> 1pi_u
   1 -->   13   29.5513  -0.0520   1sigma_g -> ???
+==================================+
 10   14.1810 eV S LAMBDA: 0.55     1Sigma_u
+-----------ALPHA-ALPHA-----------+ S=0.2715
                  [eV]      COEFF
   1 -->    2   10.2147   0.2206   1sigma_g -> 1sigma_u
   1 -->    6   13.0747   0.9559   1sigma_g -> 2sigma_u
   1 -->   10   19.9156  -0.1674   1sigma_g -> ???
   1 -->   12   27.0528  -0.0970   1sigma_g -> ???
+==================================+
 11   15.9060 eV S LAMBDA: 0.32     1Pi_g
+-----------ALPHA-ALPHA-----------+ S=0.0000
                  [eV]      COEFF
   1 -->    8   16.8567  -0.1630   1sigma_g -> 1pi_g
   1 -->    9   16.8568   0.9866   1sigma_g -> 1pi_g
+==================================+
 12   15.9082 eV S LAMBDA: 0.32     1Pi_g
+-----------ALPHA-ALPHA-----------+ S=0.0000
                  [eV]      COEFF
   1 -->    8   16.8567  -0.9866   1sigma_g -> 1pi_g
   1 -->    9   16.8568  -0.1630   1sigma_g -> 1pi_g
+==================================+
 14   16.2215 eV S LAMBDA: 0.42     1Sigma_g
+-----------ALPHA-ALPHA-----------+ S=0.0000
                  [eV]      COEFF
   1 -->    7   16.5290   0.9905   1sigma_g -> 3sigma_g
   1 -->   11   21.1435   0.1332   1sigma_g -> ???
+==================================+
 19   20.1669 eV S LAMBDA: 0.51     1Sigma_u
+-----------ALPHA-ALPHA-----------+ S=0.0563
                  [eV]      COEFF
   1 -->    2   10.2147   0.0806   1sigma_g -> 1sigma_u
   1 -->    6   13.0747   0.1327   1sigma_g -> 2sigma_u
   1 -->   10   19.9156   0.9706   1sigma_g -> ???
   1 -->   12   27.0528  -0.1835   1sigma_g -> ???
```

```
+==================================+
 20   22.6472 eV S LAMBDA: 0.67     1Sigma_g
+-----------ALPHA-ALPHA-----------+ S=0.0000
                   [eV]     COEFF
    1 -->    3   10.7754   0.0730   1sigma_g -> 2sigma_g
    1 -->    7   16.5290  -0.1301   1sigma_g -> 3sigma_g
    1 -->   11   21.1435   0.9882   1sigma_g -> ???
+==================================+
 24   28.1251 eV S LAMBDA: 0.63     1Sigma_u
+-----------ALPHA-ALPHA-----------+ S=0.1309
                   [eV]     COEFF
    1 -->    2   10.2147   0.0867   1sigma_g -> 1sigma_u
    1 -->    6   13.0747   0.1070   1sigma_g -> 2sigma_u
    1 -->   10   19.9156   0.1623   1sigma_g -> ???
    1 -->   12   27.0528   0.9763   1sigma_g -> ???
+==================================+
 25   31.2742 eV S LAMBDA: 0.77     1Pi_u
+-----------ALPHA-ALPHA-----------+ S=0.2996
                   [eV]     COEFF
    1 -->    5   12.8812   0.0582   1sigma_g -> 1pi_u
    1 -->   13   29.5513   0.8210   1sigma_g -> ???
    1 -->   14   29.5513  -0.5675   1sigma_g -> ???
+==================================+
 26   31.2758 eV S LAMBDA: 0.77     1Pi_u
+-----------ALPHA-ALPHA-----------+ S=0.2996
                   [eV]     COEFF
    1 -->    4   12.8812   0.0582   1sigma_g -> 1pi_u
    1 -->   13   29.5513   0.5675   1sigma_g -> ???
    1 -->   14   29.5513   0.8210   1sigma_g -> ???
+==================================+
 29   42.2507 eV S LAMBDA: 0.80
+-----------ALPHA-ALPHA-----------+ S=0.0000
                   [eV]     COEFF
    1 -->   15   41.8200   0.9993
+==================================+
 30   42.7558 eV S LAMBDA: 0.73
+-----------ALPHA-ALPHA-----------+ S=0.0000
                   [eV]     COEFF
    1 -->   16   42.9749   1.0000
+==================================+
```

Note how each orbital transition has the same symmetry and is consistent with the symmetry of the resultant excited state. The Λ value is a charge-transfer criterion developed by Peach, Benfield, Helgaker, and Tozer [80, 81] which can be quite useful for identifying problematic charge-transfer states whose excitation energies may be underestimated (e.g., see Ref. [82]). *Small* values of Λ (e.g., 0.20) is a sufficient (but not a necessary) condition for a charge-transfer excitation whose excitation energy may be underestimated by TD-DFT.

Now let us look at the calculated excitation energies with nonzero oscillator strengths:

State	Full	TDA	Experiment	Assignment	
2	84 800 cm^{-1} (0.2138)	85 200 cm^{-1} (0.2219)	95 160.3 cm^{-1}	$B\,^1\Sigma_u$	Lyman bands
8 & 9	103 000 cm^{-1} (0.7068)	104 000 cm^{-1} (0.7238)	99 409.18 cm^{-1}	$C\,^1\Pi_u$	Werner bands
10	114 000 cm^{-1} (0.2715)	116 000 cm^{-1} (0.3361)	110 815.65 cm^{-1}	$E\,^1\Sigma_u$	
19	163 000 cm^{-1} (0.0663)	163 000 cm^{-1} (0.0867)		$F\,^1\Sigma_u$	
24	227 000 cm^{-1} (0.1309)	229 000 cm^{-1} (0.2183)		$^1\Sigma_u$	
25 & 26	252 000 cm^{-1} (0.5992)	253 000 cm^{-1} (0.7016)		$^1\Pi_u$	

Notice the similarity of the full and TDA results. While the TDA is less subject to deficiencies in the ground state wave function, only the full calculation gives oscillator strengths obeying known sum rules. Hence only the full calculation should be used when calculating spectra. Here is a sketch of the line spectrum:

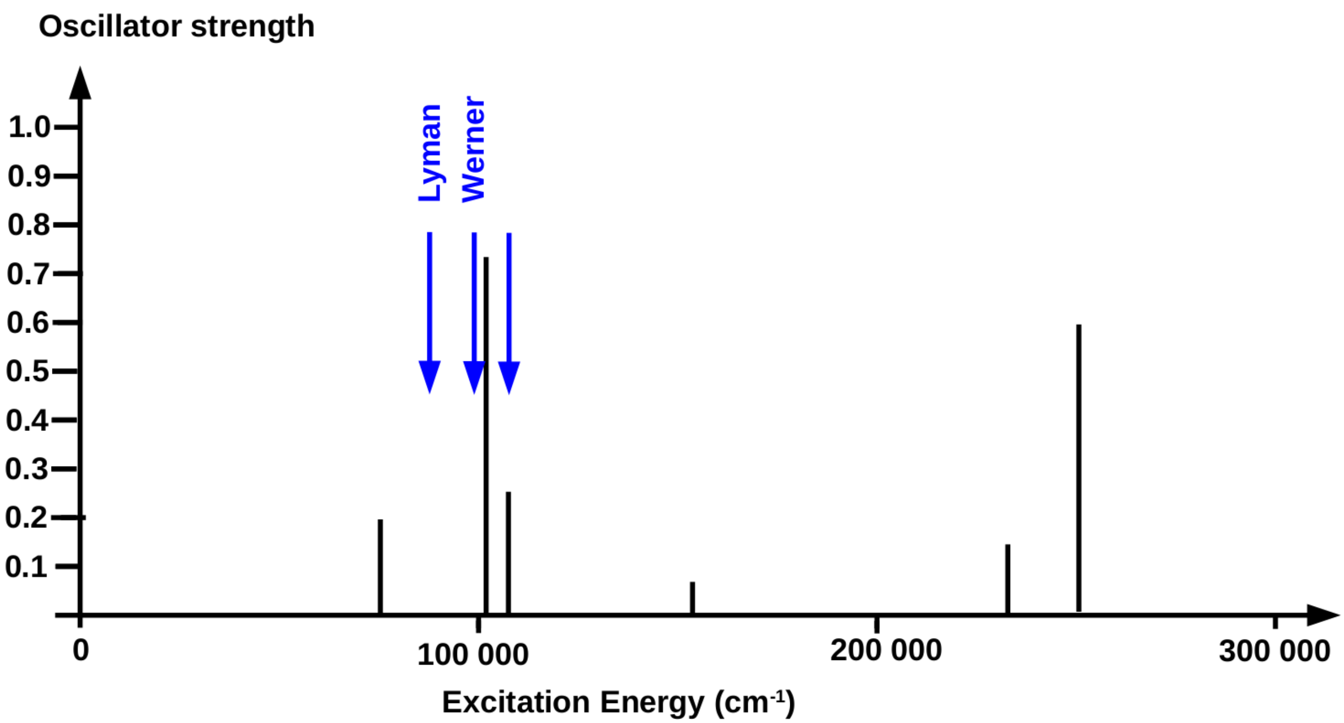

It is important, when using the Casida equation, to realize that the TD-DFT ionization threshold is at minus the negative of the highest occupied molecular orbital energy which is usually a substantional underestimation of the experimental value. In the present case, $-\epsilon_{\text{HOMO}}$ = -0.3681 Ha = 80 790 cm^{-1}. This may be compared with the experimental ionization potential which is 15.425930$\pm$0.0000027 eV [83] (0.56689 Ha = 124 418 cm^{-1}). Evidently *all* of our calculated transitions with nonzero oscillator strengths are above the TD-DFT ionization limit. This means that, while the overall shape of the absorption spectrum should be reasonably accurate, individual excitation energies are subject to variational collapse because we are effectively trying to use a finite basis set to describe the ionization continuum [84].

Finally, let us TD-DFT against the MSM:

	Triplet Energy[a]	Open-Shell Singlet Energy[a]	Multiplet Splitting
Relaxed	0.35877 Ha	–	–
MSM	0.42605 Ha	0.34777 Ha	0.07830 Ha
TD-DFT	0.34783 Ha	0.38624 Ha	0.03841 Ha
EXACT	0.39408 Ha	0.46829 Ha	0.07421 Ha

[a] Relative to the ground state energy.
Remember that the MSM uses an ENS reference, not the realxed MOs!

Very interestingly, the MSM seems to give the better value of the spin multiplet splitting in this case.

3.2 Answers for Section 2.5

3.2.1 TD-DFT and Symmetry Breaking

Here are the full TD-LDA/SAD/AUG-A3* PECs:

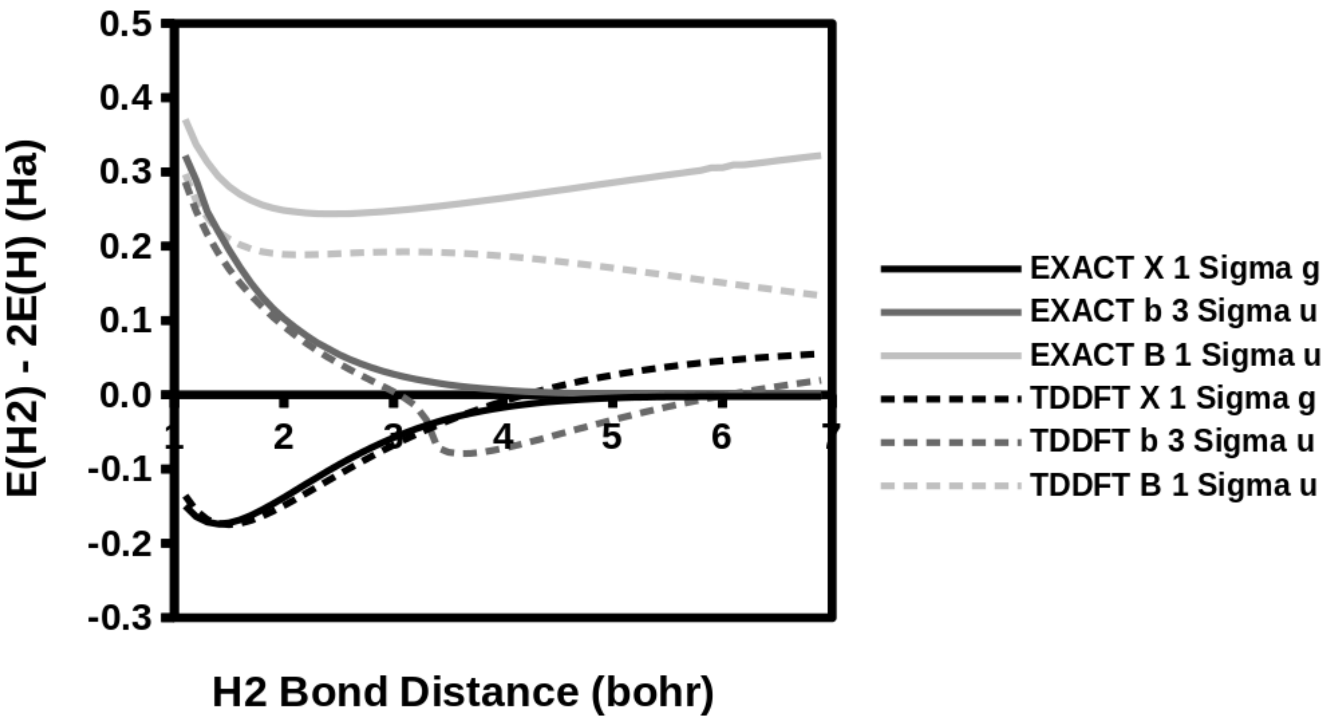

There are several things to notice here. As predicted by our VB analysis, the LDA $X\,^1\Sigma_g$ ground state curve dissociates to too high an energy.

The TD-LDA triplet curve also shows "negative" excitation energies. However, a "negative" triplet excitation energy is really just a way of representing an *imaginary* triplet excitation energy. This is called a "triplet instability". Note that the before the triplet excitation energy becomes fully imaginary, it is already going to zero indicating that there is already some problem with the way the LDA is representing the ground state. The TD-LDA open-shell singlet curve is also dissociating to too low an energy. This is a "near instability."

Here is the comparison of the LDA/SAD/AUG-A3* PECs with the EXACT GS PEC with and without symmetry breaking:

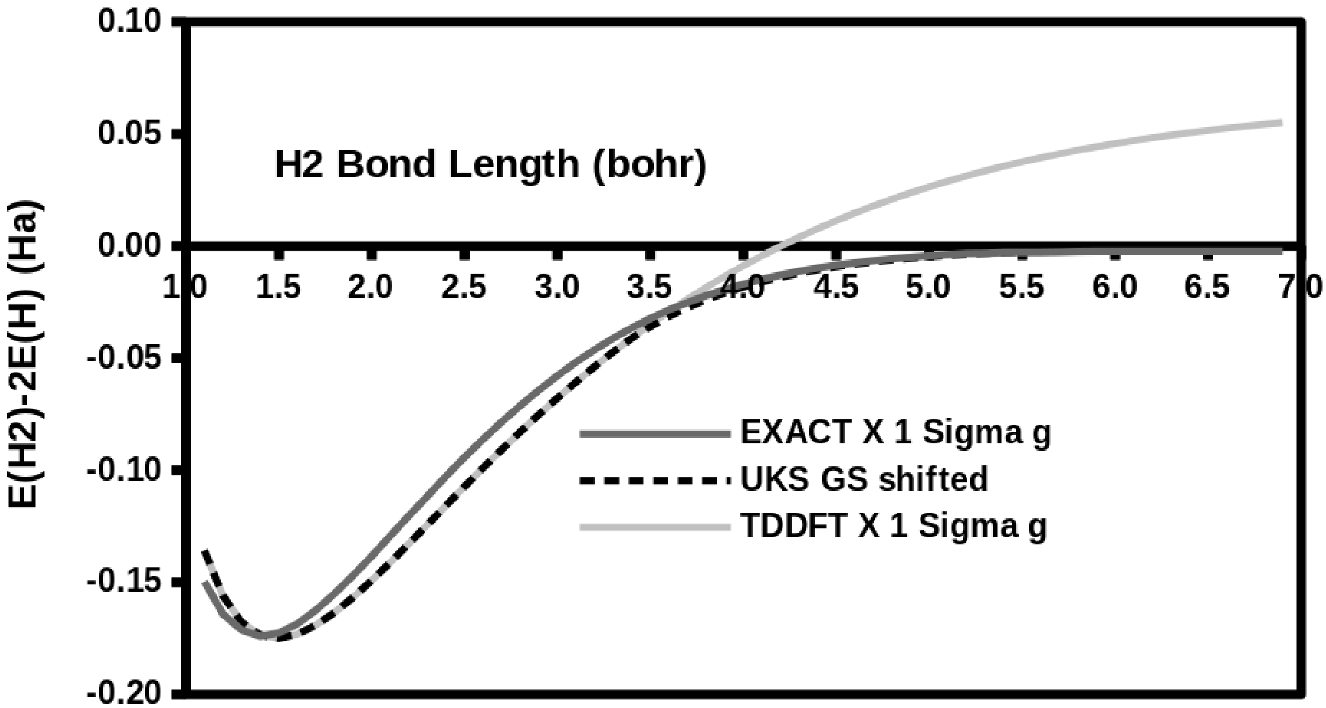

Notice how the DODS PEC becomes lower in energy than the SODS PEC at precisely the point where the triplet excitation energy becomes imaginary. This is not an accident as it can be proven mathematically (see, e.g., Ref. [70] and references therein). The bond distance where this occurs is known as the Coulson-Fischer point after an important early article in quantum chemistry [18].

> Inga Fischer-Hjalmars[85] is one of the many examples of how women have always been present in and actively contributing to our field, albeit in lesser numbers than men. Their contributions often seem to be overlooked in comparison with their male colleagues which is a shame as they may serve as important role models for women in our field!

"Correct" dissociation into [H$\uparrow$ $\downarrow$H] or [H$\downarrow$ $\uparrow$H] is observed. This is only possible because the spin-unrestricted calculation allows DODS and was one of the victories obtained by introducing spin into DFAs [86, 87] (see especially Fig. 12 of Ref. [86]).

Of course, not all is perfect, because the correct dissociation is into the singlet [H$\uparrow$ $\downarrow$H $\leftrightarrow$ H$\downarrow$ $\uparrow$H]. This problem shows up when we calculate $\langle \hat{S}^2 \rangle$ which should be equal to $S(S+1)$. For a singlet $S = 0$ so we should have $\langle \hat{S}^2 \rangle = 0$ as we do up until the Coulson-Fischer point. For a triplet $S = 1$ so we should have $\langle \hat{S}^2 \rangle = 2$. As the following graph shows, the value of $\langle \hat{S}^2 \rangle$ raises after the Coulson-Fischer point but levels out at $\langle \hat{S}^2 \rangle = 1$, indicating that we have a mixed symmetry state with 50/50 contributions from the $M_S = 0$ singlet and $M_S = 0$ triplet wave functions:

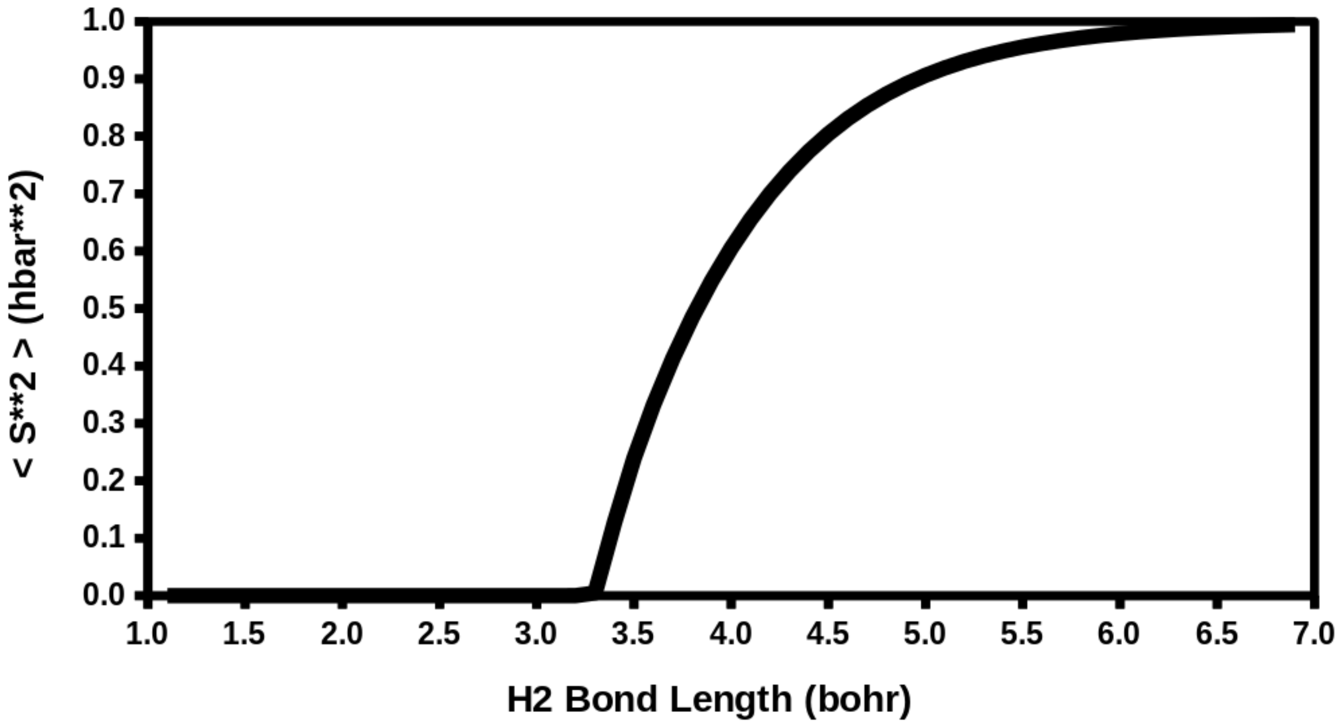

When the TDA is applied to TD Hartree-Fock (HF) calculations, we get the variational configuration interaction singles (CIS) method where each state energy is guaranteed to be an upper bound to the true state energy. While we cannot prove that the same thing will happen in TD-DFT, we certainly expect that there will be no variational collapse. Here are the TDA TD-LDA/SAD/AUG-A3* PECs:

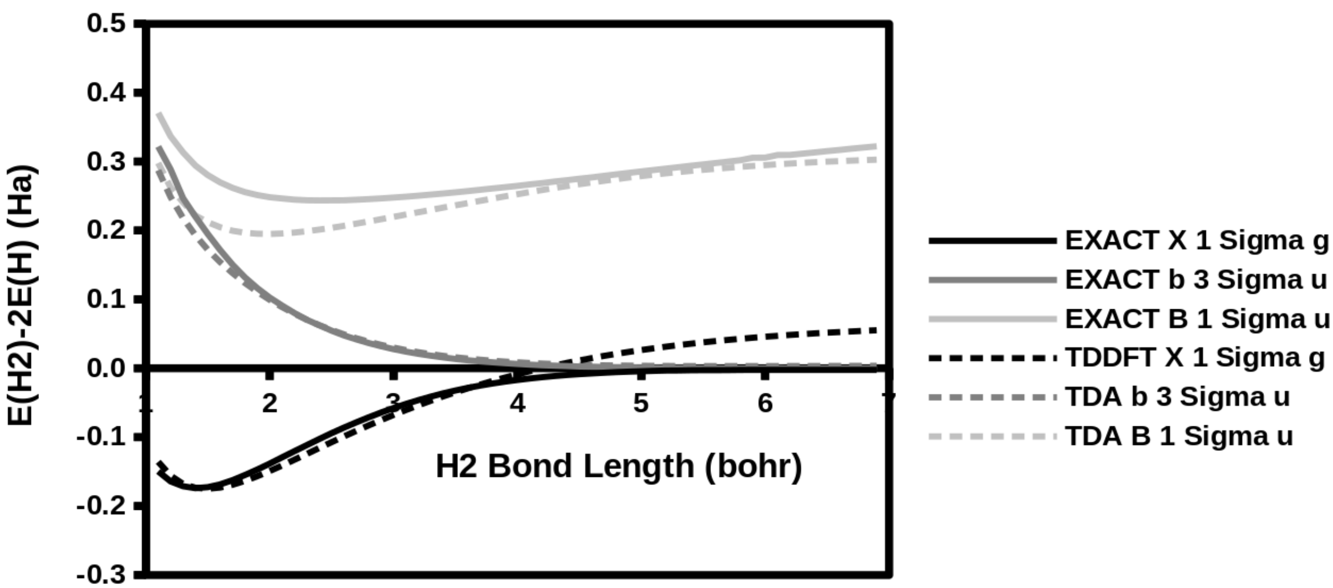

Note that we are still using the same spin-restricted KS (RKS) ground state PEC as for the full TD-DFT. It dissociates to too high an energy. But now we see that the triplet excitation with its (real valued!) negative excitation energy is dissociating correctly. Also the open-shell singlet TDA PEC is dissociating correctly. This is a major improvement if we want to study photochemical reactions rather than ultraviolet-visible (UV-Vis) absorption spectra. However the price we have to pay is that we lose the spectroscopic sum rules for the oscillator strengths.

Index

Bibliography

[1] N. B. Oozeer, A. Ponra, A. J. Etindele, and M. E. Casida, A new freely-downloadable hands-on density-functional theory workbook using a freely-downloadable version of deMon2k, Pure Appl. Chem. **95**, 213 (2023).

[2] M. E. Casida, deMon2k: Density-functional theory (DFT) for chemical physicists/physical chemists; Workbook number 1 (Abrahams workbook), http://www.demon-software.com/public_html/tutorials/main.pdf, 2022.

[3] J. S. Rowlinson, The border between physics and chemistry, Bull. Hist. Chem. **34**, 1 (2009).

[4] G. N. Lewis, The atom and the molecule, J. Am. Chem. Soc. **38**, 762 (1916).

[5] W. B. Jensen, A quantitative van Arkel diagram, J. Chem. Ed. **72**, 395 (1995).

[6] C. S. McCaw and M. A. Thompson, A new approach to chemistry education at pre-university level, Nature Chem. **1**, 95 (2009).

[7] R. Rousseau and D. Marx, Exploring the electronic structure of elemental lithium: From small molecules to nanoclusters, bulk metal, and surfaces, Chem. Eur. J. **6**, 2982 (2000).

[8] E. Schrödinger, An undulatory theory of the mechanics of atoms and molecules, Phys. Rev. **28**, 1049 (1926).

[9] E. Schrödinger, Quantisierung als Eigenwertproblem, Annalen der Physik **384**, 361 (1926).

[10] W. Heitler and F. London, Wechselwirkung neutraler Atome und homöopolare Bindung nach der Quantenmechanik, Zeitschrift für Physik **44**, 455 (1927).

[11] L. Pauling, *The Nature of the Chemical Bond*, Cornell University Press, Ithaca, NY, USA, 3rd ed., 1960 edition, 1939.

[12] G. W. Wheland, *The Theory of Resonance in Organic Chemistry and Its Application to Organic Chemistry*, Wiley, New York, 1955.

[13] G. W. Wheland, *Resonance in Organic Chemistry*, Wiley, New York, 1955.

[14] E. T. Strom, George W. Wheland: Forgotten pioneer of resonance theory, in *Pioneers of Quantum Chemistry*, edited by E. T. Strom and A. K. Wilson, volume 1122, page 75, ACS Symposium Series, 2013.

[15] G. W. Wheland, The valence-bond treatment of the oxygen molecule, Trans. Faraday Soc. **33**, 1499 (1937).

[16] P. A. M. Dirac, Quantum mechanics of many-electron systems, Proc. Roy. Soc. A **123**, 714 (1929).

[17] R. Pauncz, *Spin Eigenfunctions*, Plenum Press, New York, 1979.

[18] C. A. Coulson and I. Fischer, XXXIV. Notes on the molecular orbital treatment of the hydrogen molecule, Phil. Mag. **40**, 386 (1949).

[19] D. L. Cooper, *Valence Bond Theory*, volume 10 of *Theoretical and Computational Chemistry*, Elsevier, Amsterdam, 2002.

[20] G. A. Gallup, *Valence Bond Methods: Theory and Applications*, Cambridge University Press, Cambridge, UK, 2002.

[21] S. S. Shaik and P. C. Hiberty, *A Chemist's Guide to Valence Bond Theory*, John Wiley & Sons, Inc., Hoboken, New Jersey, USA, 2008.

[22] T. E. Sharp, Potential-energy curves for hydrogen and its ions, Atomic Data **2**, 119 (1971).

[23] T. E. Sharp, Erratum [*atomic data* **2**, 119 (1971)], Atomic Data **3**, 299 (1971).

[24] S. H. Vosko, L. Wilk, and M. Nusair, Accurate spin-dependent electron liquid correlation energies for local spin density calculations: a critical analysis, Can. J. Phys. **58**, 1200 (1980).

[25] W. Kołos and L. Wolniewicz, Potential energy curves for the $X\ ^1\Sigma_g^+$, $b\ ^3\Sigma_u^+$, and $c\ ^1\pi_u$ states of the hydrogen molecule, J. Chem. Phys. **43**, 2429 (1965).

[26] W. Kołos and L. Wolniewicz, Potentialenergy curve for the $B\ ^1\Sigma_u^+$ state of the hydrogen molecule, J. Chem. Phys. **45**, 509 (1966).

[27] W. Kołos and L. Wolniewicz, Vibrational and rotational energies for the $B\ ^1\Sigma_u^+$, $c\ ^1\pi_u$, and $a\ ^3\sigma_g^+$ states of the hydrogen molecule, J. Chem. Phys. **48**, 3672 (1968).

[28] W. Kołos and L. Wolniewicz, Theoretical investigation of the lowest doubleminimum state e, f, $^1\sigma_g^+$ of the hydrogen molecule, J. Chem. Phys. **50**, 3228 (1969).

[29] W. Kołos, *Ab initio* potential energy curves and vibrational levels for the B'', b, and b' states of the hydrogen molecule, J. Mol. Spectrosc. **62**, 429 (1976).

[30] W. Kołos and J. Rychlewski, Ab initio potential energy curves and vibrational levels for the C and $D\ ^1\Pi_u$ states of the hydrogen molecule, J. Mol. Spectrosc. **62**, 109 (1976).

[31] W. Kołos and J. Rychlewski, Ab initio potential energy curves and vibrational levels for the c, l, and i states of the hydrogen molecule, J. Mol. Spectrosc. **66**, 428 (1977).

[32] L. Wolniewicz and K. J. Dressler, The $B\ ^1\Sigma_u^+$, $B'\ ^1\Sigma_u^+$, $C\ ^1\Pi_u$, and $D\ ^1\Pi_u$ states of the H_2 molecule. Matrix elements of angular and radial nonadiabatic coupling and improved ab initio potential energy curves, Chem. Phys. **88**, 3861 (1988).

[33] G. Staszewska and L. Wolniewicz, Adiabatic energies of excited $^1\Sigma_u$ states of the hydrogen molecule, J. Mol. Spectrosc. **212**, 208 (2002).

[34] L. Wolniewicz and G. Staszewska, Excited $^1\Pi_u$ and the $^1\Pi_u rightarrow\ X\ ^1\Sigma_g^+$ transition moments of the hydogen molecule, J. Mol. Spectrosc. **220**, 45 (2003).

[35] C. Lee, Y. Gim, and T. H. Choi, Calculation of potential energy curves of excited states of molecular hydrogen by multi-reference configuration-interaction method, Bull. Korean Chem. Soc. **34**, 1771 (2013).

[36] E. R. Davidson and D. Feller, Basis set selection for molecular calculations, Chem. Rev. **86**, 681 (1986).

[37] J. G. Hill, Gaussian basis sets for molecular applications, Int. J. Quant. Chem. **113**, 21 (2013).

[38] B. Delley, An allelectron numerical method for solving the local density functional for polyatomic molecules, J. Chem. Phys. **92**, 508 (1990).

[39] J. C. Slater, Atomic shielding constants, Phys. Rev. **36**, 57 (1930).

[40] G. te Velde, F. M. Bickelhaupt, E. J. Baerends, C. F. Guerra, S. J. A. van Gisbergen, J. G. Snijders, and T. Ziegler, Chemistry with ADF, J. Comput. Chem. **22**, 931 (2001).

[41] N. Godbout, D. R. Salahub, J. Andzelm, and E. Wimmer, Optimization of Gaussian-type basis sets for local spin density functional calculations. Part I. Boron through neon, optimization technique and validation, Can. J. Phys. **70**, 560 (1992).

[42] P. Calaminici, F. Janetzko, A. M. Köster, R. Mejia-Olvera, and B. Zuñ-Gutierrez, Density functional theory optimized basis sets for gradient corrected functionals: $3d$ transition metal systems, J. Chem. Phys. **126**, 044108 (2007).

[43] W. J. Hehre, R. Ditchfield, R. F. Stewart, and J. A. Pople, Selfconsistent molecular orbital methods. IV. Use of Gaussian expansions of Slater-type orbitals. Extension to secondrow molecules, J. Chem. Phys. **52**, 2769 (1970).

[44] P. C. Hariharan and J. A. Pople, The influence of polarization functions on molecular orbital hydrogenation energies, Theor. Chim. Acta **28**, 213 (1973).

[45] M. M. Francl, W. J. Pietro, and W. J. Hehre, Selfconsistent molecular orbital methods. XXIII. A polarization-type basis set for secondrow elements, J. Chem. Phys. **77**, 3654 (1982).

[46] R. Krishnan, J. S. Binkley, R. Seeger, and J. A. Pople, Selfconsistent molecular orbital methods. XX. A basis set for correlated wave functions, J. Chem. Phys. **72**, 650 (1980).

[47] F. Weigend and R. Ahlrichs, Balanced basis sets of split valence, triple zeta valence and quadruple zeta valence quality for H to Rn: Design and assessment of accuracy, Phys. Chem. Chem. Phys. **7**, 3297 (2005).

[48] N. Rega, M. Cossi, and V. Barone, Development and validation of reliable quantum mechanical approaches for the study of free radicals in solution, J. Chem. Phys. **105**, 11060 (1996).

[49] S. Huzinaga, Gaussian-type functions for polyatomic systems. I, J. Chem. Phys. **42**, 1293 (1965).

[50] G. C. Lie and E. Clementi, Study of the electronic structure of molecules. XXI. Correlation energy corrections as a functional of the Hartree-Fock density and its application to the hydrides of the second row atoms, J. Chem. Phys. **60**, 1275 (1974).

[51] A. J. Sadlej, Medium-size polarized basis sets for high-level correlated calculations of molecular electric properties, Collection Czech. Chem. Commun. **53**, 1995 (1988).

[52] J. Guan, P. Duffy, J. T. Carter, D. P. Chong, K. C. Casida, M. E. Casida, and M. Wrinn, Comparison of local-density and Hartree-Fock calculations of molecular polarizabilities and hyperpolarizabilities, J. Chem. Phys. **98**, 4753 (1993).

[53] R. Pu-Amérigo, M. Merchán, I. Nebot-Gil, P. Widmark, and B. O. Roos, Density matrix averaged atomic natural orbital (ANO) basis sets for correlated molecular wave functions. III. First row transition metal atoms, Theor. Chim. Acta **92**, 149 (1995).

[54] D. E. Woon and T. H. D. Jr., Gaussian basis sets for use in correlated molecular calculations. V. Core-valence basis sets for boron through neon, J. Chem. Phys. **103**, 4572 (1995).

[55] T. H. D. Jr., Gaussian basis sets for use in correlated molecular calculations. I. The atoms boron through neon and hydrogen, J. Chem. Phys. **90**, 1007 (1989).

[56] F. Jensen, The basis set convergence of spin-spin coupling constants calculated by density functional methods, J. Chem. Theo. Comp. **2**, 1360 (2006).

[57] T. H. Dunning and P. J. Hay, Gaussian basis sets for molecular calculations, in *Methods of Electronic Structure Theory*, edited by H. F. S. III, volume 3 of *Modern Theoretical Chemistry*, page 1, Springer, 1977.

[58] I. Cherkes, S. Klaiman, and N. Moiseyev, Spanning the Hilbert space with an even tempered gaussian basis set, Int. J. Quant. Chem. **109**, 2996 (2009).

[59] T. Ziegler, A. Rauk, and E. J. Baerends, On the calculation of multiplet energies by the Hartree-Fock-Slater method, Theor. Chim. Acta **4**, 877 (1977).

[60] A. Szabo and N. S. Ostlund, *Modern Quantum Chemistry: Introduction to Advanced Electronic Structure Theory*, McMillan, New York, 1982.

[61] A. Ponra, A. J. Etindele, O. Motapon, and M. E. Casida, Practical treatment of singlet oxygen with density-functional theory and the multiplet-sum method, Theo. Chem. Acc. **140**, 154 (2021).

[62] M. E. Casida, Time-dependent density-functional response theory for molecules, in *Recent Advances in Density Functional Methods, Part I*, edited by D. P. Chong, page 155, World Scientific, Singapore, 1995.

[63] R. Bauernschhmitt and R. Ahlrichs, Treatment of electronic excitations within the adiabatic approximation of time dependent density functional theory, Chem. Phys. Lett. **256**, 454 (1996).

[64] C. Jamorski, M. E. Casida, and D. R. Salahub, Dynamic polarizabilities and excitation spectra from a molecular implementation of time-dependent density-functional response theory: N_2 as a case study, J. Chem. Phys. **104**, 5134 (1996).

[65] J. Carmona-Espindola and A. M. Köster, Photoabsorption spectra from time-dependent auxiliary density functional theory, Can. J. Chem. **91**, 795 (2013).

[66] L. Hernández-Segura and A. M. Köster, Efficient implementation of time-dependent auxiliary density functional theory, J. Chem. Phys. **158**, 024108 (2023).

[67] M. E. Casida, A. Ipatov, and F. Cordova, Linear-response time-dependent density-functional theory for open-shell molecules, in *Time-Dependent Density-Functional Theory*, edited by M. A. L. Marques, C. Ullrich, F. Nogueira, A. Rubio, and E. K. U. Gross, Lecture Notes in Physics, page 243, Springer, Berlin, 2006.

[68] A. Ipatov, A. Fouqueau, C. P. del Valle, F. Cordova, M. E. Casida, A. M. Köster, A. Vela, and C. J. Jamorski, Excitation energies from an auxiliary-function formulation of time-dependent density-functional response theory with charge conservation constraint, J. Molec. Struct. (Theochem) **762**, 179 (2006).

[69] S. Hirata and M. Head-Gordon, Time-dependent density functional theory within the Tamm-Dancoff approximation, Chem. Phys. Lett. **314**, 291 (1999).

[70] M. E. Casida, F. Gutierrez, J. Guan, F. Gadea, D. R. Salahub, and J. Daudey, Charge-transfer correction for improved time-dependent local density approximation excited-state potential energy curves: Analysis within the two-level model with illustration for H_2 and LiH, J. Chem. Phys. **113**, 7062 (2000).

[71] A. Campargue, S. Kassi, K. Pachucki, and J. Komasa, The absorption spectrum of H_2: CRDS measurements of the (2-0) band, review of the literature data and accurate *ab initio* line list up to 35 000 cm^{-1}, Phys. Chem. Chem. Phys. **14**, 802 (2012).

[72] T. Namioka, Absorption spectra of H_2 in the vacuum-ultraviolet region. I. the Lyman and the Werner bands, J. Chem. Phys. **40**, 3154 (1964).

[73] I. Dabrowski and G. Herzberg, The absorption spectrum of D_2 from 1100 to 840 å, Can. J. Phys. **52**, 74 (1974).

[74] C. A. Coulson, *Valence*, Clarendon Press, Oxford, England, UK, 1952.

[75] A. Ponra, C. Bakasa, A. J. Etindele, and M. E. Casida, Diagrammatic multiplet-sum method (MSM) density-functional theory (DFT): Investigation of the transferability of integrals in "simple" DFT-based approaches to multi-determinantal problems, J. Chem. Phys. **159**, 244306 (2023).

[76] M. E. Casida, A. Ponra, C. Bakasa, and A. J. Etindele, Diagrammatic multiplet-sum method (MSM) density-functional theory (DFT): Completion of the two-orbital two-electron model (TOTEM) with an application to the avoided crossing in lithium hydride (LiH), J. Chem. Phys. **162**, 144317 (2025).

[77] B. Schaftenaar, MOLDEN: A pre- and post processing program of molecular electronic structure, https://www3.cmbi.umcn.nl/molden/, Last accessed 22 May 2021.

[78] G. Schaftenaar and J. H. Noordik, MOLDEN: a pre- and post-processing program for molecular and electronic structures, J. Comput. Aided Mol. Des. **14**, 123 (2000).

[79] G. Schaftenaar, E. Vlieg, and G. Vriend, MOLDEN 2.0: quantum chemistry meets proteins, J. Comput. Aided Mol. Des. **31**, 789 (2017).

[80] M. J. G. Peach, P. Benfield, T. Helgaker, and D. J. Tozer, Excitation energies in density functional theory: An evaluation and a diagnostic test, J. Chem. Phys. **128**, 044118 (2008).

[81] M. J. G. Peach and D. J. Tozer, Illustration of a TDDFT spatial overlap diagnostic by basis function exponent scaling, J. Mol. Struct.: THEOCHEM **914**, 110 (2009).

[82] O. Valsson, C. Filippi, and M. E. Casida, Regarding the use and misuse of retinal protonated Schiff base photochemistry as a test case for time-dependent density-functional theory, J. Chem. Phys. **140**, 144104 (2015).

[83] E. E. Eyler, R. C. Short, and F. M. Pipkin, Precision spectroscopy of the nf triplet Rydberg states of H_2 and determination of the triplet ionization potential, Phys. Rev. Lett. **56**, 2602 (1986).

[84] M. E. Casida, C. Jamorski, K. C. Casida, and D. R. Salahub, Molecular excitation energies to high-lying bound states from time-dependent density-functional response theory: Characterization and correction of the time-dependent local density approximation ionization threshold, J. Chem. Phys. **108**, 4439 (1998).

[85] A. J. Johansson, Inga Fischer-Hjalmars (19182008): Swedish pharmacist, humanist, and pioneer quantum chemist, J. Chem. Ed. **89**, 1274 (2012).

[86] O. Gunnarsson and B. I. Lundqvist, Exchange and correlation in atoms, molecules, and solids by the spin-density-functional formalism, Phys. Rev. B **13**, 4274 (1976).

[87] O. Gunnarsson and B. I. Lundqvist, Erratum: Exchange and correlation in atoms, molecules, and solids by the spin-density-functional formalism, Phys. Rev. B **15**, 6006 (1977).